

The role of ADP-ribosylation in regulating DNA interstrand crosslink repair

Alasdair R. Gunn^{1, 5}, Benito Banos-Pinero^{2, 5}, Peggy Paschke^{1,*}, Luis Sanchez-Pulido³, Antonio Ariza², Joseph Day¹, Mehera Emrich¹, David Leys⁴, Chris P. Ponting³, Ivan Ahel^{2, 6} and Nicholas D. Lakin^{1, 6}

¹Department of Biochemistry, University of Oxford, South Parks Road, Oxford, UK

²Dunn School of Pathology, University of Oxford, South Parks Road, Oxford, UK

³MRC Human Genetics Unit, The MRC Institute of Genetics and Molecular Medicine, University of Edinburgh, Western General Hospital, Crewe Road, Edinburgh EH4 2XU, Scotland, UK

⁴Manchester Institute of Biotechnology, University of Manchester, Princess Street 131, Manchester, UK

* Current address: MRC Laboratory of Molecular Biology, Francis Crick Avenue, Cambridge Biomedical Campus, Cambridge, CB2 0QH

⁵Joint first authors

⁶Corresponding authors

Tel: (+44) 1865 613244

Email: nicholas.lakin@bioch.ox.ac.uk

ivan.ahel@path.ox.ac.uk

Keywords: *Dictyostelium*/ ADP-ribosyltransferases/ PARPs/ Interstrand crosslink

SUMMARY STATEMENT

ADP-ribosylation is a post-translation modification required to mediate the cellular response to several forms of DNA damage. Here, we identify a role for ADP-ribosylation in response to DNA interstrand crosslinks.

ABSTRACT

ADP-ribosylation by ADP-ribosyltransferases (ARTs) has a well-established role in DNA strand break repair by promoting enrichment of repair factors at damage sites through ADP-ribose interaction domains. Here we exploit the simple eukaryote *Dictyostelium* to uncover a role for ADP-ribosylation in regulating DNA interstrand crosslink repair and redundancy of this pathway with non-homologous end-joining (NHEJ). *In silico* searches identify a protein that contains a permuted macrodomain (Aprataxin/APLF-and-PNKP-Like protein; APL). Structural analysis reveals permuted macrodomains retain features associated with ADP-ribose interactions and APL is capable of binding poly-ADP-ribose through its macrodomain. APL is enriched in chromatin in response to cisplatin, an agent that induces DNA interstrand crosslinks (ICLs). This is dependent on the macrodomain of APL, and the ART Adprt2, indicating a role for ADP-ribosylation in the cellular response to cisplatin. Although *adprt2*⁻ cells are sensitive to cisplatin, ADP-ribosylation is evident in these cells due to redundant signalling by the DSB-responsive ART Adprt1a, promoting NHEJ-mediated repair. These data implicate ADP-ribosylation in DNA ICL repair and identify NHEJ can function to resolve this form of DNA damage in the absence of Adprt2.

INTRODUCTION

ADP-ribosyltransferases (ARTs) catalyse the addition of single or poly-ADP ribose moieties onto target proteins by mono-ADP ribosylation (MARylation) or poly-ADP ribosylation (PARylation) respectively (Gibson and Kraus, 2012; Vyas et al., 2014). ARTs are conserved in a wide variety of organisms, with 17 genes containing predicted ART domains being identified in humans (Hottiger et al., 2010). PARP1 and PARP2, the founder members of the ART family, in addition to PARP5a and PARP5b are poly-ARTs. All other active ARTs catalyse MARylation (Vyas et al., 2014). ADP-ribosylation has been implicated in a wide variety of cellular processes including cell growth and differentiation, transcriptional regulation and programmed cell death (Hottiger et al., 2010; Messner and Hottiger, 2011; Quenet et al., 2009).

The best defined role of ARTs is in DNA repair, particularly of DNA strand breaks. PARP1 is recruited to and activated by DNA single strand breaks (SSBs) and modifies a variety of substrates, including itself, proximal to the DNA lesion (Caldecott, 2008; Krishnakumar and Kraus, 2010). PARP1 is required for resolution of SSBs and disruption of its activity results in delayed repair and sensitivity to agents that induce base alkylation or DNA strand breaks (de Murcia et al., 1997; Ding et al., 1992; Fisher et al., 2007; Le Page et al., 2003; Masutani et al., 1999; Trucco et al., 1998). The finding that PARP2 catalyses residual PARylation in *parp1*^{-/-} cells led to the proposal that this ART also functions in SSB repair (Ame et al., 1999). Consistent with this model, *parp2*^{-/-} mice are sensitive to DNA damaging agents that induce strand breaks, in addition to displaying increased chromosome instability and delayed repair of damage following exposure to DNA alkylating agents (Menissier de Murcia et al., 2003; Schreiber et al., 2002). Although the relationship between PARP1 and PARP2 in regulating SSB repair is unclear, redundancy between these ARTs is implied by the embryonic lethality of *parp1*^{-/-}*parp2*^{-/-} mice (Menissier de Murcia et al., 2003).

ARTs are also critical for resolution of DNA double strand breaks (DSBs) by homologous recombination (HR) or non-homologous end-joining (NHEJ). PARP1 and PARP2 have been implicated in HR, particularly with reference to restart of stalled or damaged replication forks (Bryant et al., 2009; Sugimura et al., 2008; Yang et al., 2004). PARP1 is also required for alternative-NHEJ (A-NHEJ), an end-joining pathway activated in the absence of core NHEJ factors (Audebert et al., 2004; Brown et al., 2002; Robert et al., 2009; Wang et al., 2006). However, there are conflicting reports regarding the requirement for PARP1 in classic NHEJ (Luijsterburg et al., 2016; Yang et al., 2004). Instead, PARP3 PARylates targets at DSBs and promotes NHEJ by facilitating accumulation of repair factors such as APLF and Ku at

damage sites (Boehler et al., 2011; Couto et al., 2011; Loseva et al., 2010; Rulten et al., 2011).

A unifying theme of how ADP-ribosylation regulates resolution of DNA strand breaks, and possibly other varieties of DNA lesion, is through promoting the assembly of DNA repair and chromatin remodelling factors at damage sites. This is achieved through ADP-ribose interaction domains in these factors that interact with proteins PARylated or MARylated at DNA lesions. The best characterised of these modules include a 20 amino acid PAR binding motif (PBM), PAR-binding zinc-finger (PBZ), macro and WWE domains (Gibson and Kraus, 2012). The PBM was the first ADP-ribose binding module to be identified and is present in a number of proteins, including several DDR factors (Gagne et al., 2008). PBZ domains are apparent in three vertebrate proteins, all of which have been implicated in the DDR, and are required to enrich CHFR and APLF at DNA damage sites (Ahel et al., 2008; Rulten et al., 2011). Whilst PBZ domains bind ADP-ribose polymers, macrodomains are more diverse in nature, binding a variety of ligands including PAR chains, mono-ADP-ribose units and O-acetyl ADP-ribose (Aravind, 2001; Han et al., 2011; Karras et al., 2005; Rack et al., 2016). Additionally, some macrodomains possess PAR and MAR-hydrolase activity, implicating these proteins in the removal of ADP-ribose moieties to regulate a variety of cellular processes (Barkauskaite et al., 2015; Jankevicius et al., 2013; Rosenthal et al., 2013; Sharifi et al., 2013; Slade et al., 2011). Despite this functional diversity, macrodomains uniformly adopt an $\alpha/\beta/\alpha$ sandwich fold, with amino acid variations within a conserved binding pocket being responsible for the ligand-binding specificity or catalytic activity of each domain. Macrodomains have been identified in several DDR proteins and are required to recruit the chromatin remodelling factor ALC1 and the histone variant macroH2A1.1 to DNA damage (Ahel et al., 2009; Gottschalk et al., 2009; Timinszky et al., 2009).

Previously, we and others identified that the genetically tractable eukaryote *Dictyostelium discoideum* contains several DNA repair proteins that are absent or show limited conservation in other invertebrate model organisms (Block and Lees-Miller, 2005; Hsu et al., 2006; Hudson et al., 2005; Zhang et al., 2009). In this regard, several ARTs are apparent in the *Dictyostelium* genome (Pears et al., 2012), and similar to vertebrates we find that two (Adprt1b and Adprt2) confer cellular resistance to SSBs (Couto et al., 2011). A third ART (Adprt1a) is dispensable for SSB repair, but instead promotes NHEJ by facilitating accumulation of Ku at DSBs (Couto et al., 2011; Pears et al., 2012). Interestingly, the PBZ domain is unusually prevalent in *Dictyostelium*, with seven proteins containing this domain compared to three in vertebrates (Ahel et al., 2008). *Dictyostelium* Ku70 contains a PBZ domain which is required to enrich the protein in chromatin following DNA DSBs and

promote efficient NHEJ (Couto et al., 2011). Given this motif is absent in vertebrate Ku70, these observations suggest that PBZ domains have been fused to a number of *Dictyostelium* DNA repair proteins during evolution. Therefore, the presence of other ADP-ribose interaction domains may act as a surrogate marker for novel proteins involved in the DNA damage response (DDR).

Whilst the role of ARTs in DNA strand break repair is well established, whether these enzymes regulate other repair processes remains unclear. Here we exploit the increased frequency of ADP-ribose interaction motifs in *Dictyostelium* to uncover a role for ADP-ribosylation in regulating repair of DNA damage inflicted by cisplatin, an agent that induces DNA interstrand crosslinks (ICLs). Through an *in silico* approach to identify novel macrodomain containing proteins in this organism, we identify a protein containing regions of homology to Aprataxin, APLF and PNKP that we have called APL (Aprataxin/APLF-and-PNKP-Like protein). APL is recruited to DNA damage induced by cisplatin, in a manner that is dependent on its macrodomain. Consistent with these observations, we report that ADP-ribosylation is induced in response to cisplatin, and that ARTs are required for tolerance to DNA damage induced by this agent. Finally, we exploit the genetic tractability of *Dictyostelium* to uncover novel redundancy between ARTs and the NHEJ pathway in allowing cells to tolerate cisplatin exposure.

RESULTS

Identification of novel *Dictyostelium* macrodomain-containing proteins

Previous bioinformatics analysis indicates an increased frequency of PBZ domain-containing proteins in *Dictyostelium* relative to humans (Ahel et al., 2008). The majority of these proteins are orthologues of vertebrate factors previously implicated in the DDR. We hypothesised that this may also be the case for other ADP-ribose-binding modules, and thus the presence of these domains will serve as surrogate markers for novel DDR proteins. Although ADP-ribose-binding macrodomains have been identified in human DNA repair proteins (Ahel et al., 2009; Nicolae et al., 2015), these modules are evolutionarily diverse and exhibit a high level of primary sequence divergence that hinders their identification and annotation (Rack et al., 2016). Therefore, we sought to identify previously unannotated *Dictyostelium* macrodomain-containing proteins in the hope that this would uncover novel proteins with a role in the DDR. Accordingly, we performed a genome-wide search using the primary sequence of known human macrodomains as the starting point for homology detection and subsequent generation of profile hidden Markov models (profile-HMMs) (Eddy, 1998). Profile-HMMs are mathematical constructs that incorporate the amino acid variation at each position in a multiple sequence alignment of a domain family, thereby providing more sensitivity than performing homology searches with an input of a single sequence. Given we sought to identify ADP-ribose-binding domains, we used the sequence of macrodomains known to interact with ADP-ribose in our searches, such as that found in ALC1 (Ahel et al., 2009). This approach yielded six *Dictyostelium* proteins with macrodomains, three of which were not previously annotated in protein databases (Fig. 1A).

One of the unannotated macrodomain containing proteins is the *Dictyostelium* orthologue of DNA Ligase III. Given that vertebrate DNA ligase III does not contain a macrodomain, this supports our hypothesis that these modules can act as markers for DNA repair proteins in *Dictyostelium*. A further protein identified in this screen (Q54B72, DDB_G0293866) contains a macrodomain at its C-terminus, a central PBZ domain with predicted PAR-binding activity, in addition to an N-terminal FHA-like domain similar to those found in the human DNA repair proteins Aprataxin, APLF and PNKP (Fig. 1A,B) (Ali et al., 2009; Chappell et al., 2002; Clements et al., 2004; Iles et al., 2007). Given the similarity of this protein to Aprataxin, APLF and PNKP, we called this factor Aprataxin/APLF-and-PNKP-Like protein (APL). Interestingly, the N- and C- termini of the APL macrodomain align with the C- and N- termini of human macrodomains respectively (Fig. S1), indicating it has undergone a circular permutation during evolution (Ponting and Russell, 1995). This circularly permuted macrodomain was found to be present in orthologues of APL in other dictyostelids (Fig. 1B). Such a permutation involving gross rearrangements of the primary sequence could result in

severe tertiary structural alterations, impacting on the functionality of the macrodomain. Therefore, we assessed whether or not this circular permutation has affected the functional structure of the domain. Firstly, we investigated if this permutation was a unique event in dictyostelids, or one that is evolutionarily conserved across other species, thereby providing evidence that it may be required for a biological function. A BLAST database search with the macrodomain sequence of APL identifies the permuted macrodomain in a small number of other organisms, including the plants *Arabidopsis thaliana* and *Oryza sativa*. These permuted domains show a high level of primary sequence conservation with that found in APL (Fig. 2A), indicating that the same permuted macrodomain is present in several diverse species and implying that it is functionally important.

In order to assess whether these permuted macrodomains retain important structural characteristics, we solved the X-ray crystal structures of the isolated permuted macrodomains found in *Dictyostelium* APL and *O. sativa* Q10MW4 (Fig. 2B,C and Table S1). Selenomethionine-substituted protein of the *Dictyostelium* macrodomain was used to collect single wavelength anomalous diffraction X-ray data, which was phased with AUTOSOL (Terwilliger et al., 2009). Subsequently, X-ray data of the *O. sativa* macrodomain was solved via molecular replacement with PHASER (Storoni et al., 2004) by using the *Dictyostelium* macrodomain structure as the search model. Previously solved structures of classical macro domains indicate that they consist of a non-parallel β -sheet core flanked by α -helices, with a cleft forming the binding pocket for ADP-ribose (Rack et al., 2016). These structural features are conserved in the permuted macrodomain found in *Dictyostelium* APL (Fig. 2B), indicating that the permutation does not drastically alter the structure of the domain. We were able to obtain the *O. sativa* macrodomain in a complex with ADP-ribose (Fig. 2C), further confirming that the canonical mode of interaction with ADP-ribose is also retained. For example, the acidic amino acids D175 (E439 in *Dictyostelium*) that forms hydrogen bonds with the ADP-ribose ligand, and the aromatic F113 that forms the binding pocket for the distal ribose unit are found in *O. sativa* Q10MW4 and canonical macrodomains, suggesting that these amino acids will perform the same functions in most macrodomains (Ahel et al., 2009).

To more formally assess whether APL is indeed an ADP-ribose-binding protein, and which domains of this protein are responsible, we expressed and purified a GST-tagged form of APL (GST-APL) and tested its ability to bind PAR polymers *in vitro* utilising a slot blot assay. Consistent with a previous report (Couto et al., 2011), a C-terminal region of Ku70 displayed PAR-binding activity in this assay that is dependent on its PBZ domain (Fig. 2D). Importantly, GST-APL also binds PAR, indicating that this protein is able to interact with

ADP-ribose polymers *in vitro*. Given APL contains both PBZ and macrodomains capable of interacting with ADP-ribose polymers, we next determined which domains of APL are responsible for PAR-binding by assessing their ability to interact with PAR *in vitro*. Whilst the FHA domain of APL exhibits limited ability to interact with PAR *in vitro*, both the macro and PBZ domains of APL interact with ADP-ribose polymers (Fig. 2E). Taken together, these data indicate that APL is indeed able to interact with PAR *in vitro* and that both the PBZ and macrodomains of the protein are able to perform this function.

The macrodomain is required to enrich APL on chromatin in response to cisplatin-induced DNA damage

The N-terminal FHA domain of APL is most similar to those that facilitate the interaction of Aprataxin, APLF and PNKP with the DNA repair proteins XRCC1 and XRCC4 (Ali et al., 2009; Chappell et al., 2002; Clements et al., 2004; Iles et al., 2007). Taken together with the presence of a PBZ domain, a motif present in proteins that function in the DDR, this suggests a role for APL in DNA repair. To investigate this, we generated a strain disrupted in the *apl* gene (Fig. S2) and assessed whether recombinant Myc-tagged APL expressed in these cells was enriched in chromatin following exposure to a specific form of genotoxic stress. No significant enrichment of Myc-APL was observed in chromatin fractions prepared from cells exposed to agents that induce base damage (methyl methanesulphonate; MMS), DNA DSBs (phleomycin) or bulky adducts repaired by nucleotide excision repair (4-nitroquinoline-1-oxide; 4-NQO), despite the induction of DNA damage under these conditions, as judged by elevated γ H2AX (Fig. 3A). Strikingly, however, we observed elevated levels of Myc-APL in chromatin fractions following exposure to the DNA ICL-inducing agent cisplatin, implicating APL in the response to DNA damage inflicted by this agent.

To determine whether the macrodomain of APL is required for this function, we generated a Myc-tagged form of APL with the macrodomain deleted and assessed its ability to assemble in chromatin following DNA damage. As observed previously, wild-type APL is effectively enriched in chromatin following exposure of cells to cisplatin (Fig. 3B). Strikingly, deletion of the macrodomain almost totally eliminates enrichment of APL in chromatin in response to cisplatin. Taken together, these data indicate APL as a novel sensor for cisplatin-induced DNA damage and that the macrodomain of this protein is required for this function.

Nuclear ADP-ribosylation is induced following cisplatin treatment

Although the role of ARTs in SSB and DSB repair is well established, whether these enzymes are required for repair of other varieties of DNA lesion such as DNA ICLs is

unknown. Our data indicating the macrodomain of APL interacts with ADP-ribose polymers *in vitro*, taken together with the requirement of this domain to enrich APL in chromatin following exposure of cells to cisplatin, implicates ADP-ribosylation in the cellular response to DNA ICLs. To assess this possibility, we investigated whether ADP-ribosylation is induced in response to cisplatin. Ax2 cells were exposed to increasing doses of cisplatin, and ADP-ribosylation in whole cell extracts assessed by western blotting with reagents that detect both MARYlation and PARylation (Fig. 4A). We observe a dose-dependent increase in ADP-ribosylated proteins in cells, indicating that cisplatin does induce cellular ADP-ribosylation. Moreover, consistent with ADP-ribosylation being induced at DNA damage sites, we observe the formation of ADP-ribosylation nuclear foci in a time-dependent manner, with 81% of cells containing greater than 3 foci after 8 hours of cisplatin treatment (Fig. 4B). Pre-treatment of Ax2 cells with PARP inhibitors that inhibit ADP-ribosylation in *Dictyostelium* (Couto et al., 2011) significantly reduces the number of nuclei exhibiting ADP-ribosylation (Fig. 4C), indicating *Dictyostelium* ARTs are activated in response to cisplatin-treatment.

Adprt1a-mediated NHEJ is required for tolerance of cisplatin-induced DNA damage in the absence of Adprt2

We wished to identify the ARTs responsible for cisplatin-induced ADP-ribosylation. Similar to humans, two *Dictyostelium* ARTs (Adprt1b and Adprt2) are required for tolerance of cells to DNA SSBs, whilst a third ART (Adprt1a) is required to promote NHEJ of DNA DSBs (Couto et al., 2013; Couto et al., 2011). We therefore considered whether any of these ARTs are similarly required for the cellular response to cisplatin. APL enrichment in chromatin following cisplatin exposure is dependent on the macrodomain of the protein (Fig. 3B), suggesting that ART-mediated ADP-ribosylation regulates this process. Therefore, we initially tested whether cisplatin-induced enrichment of APL in chromatin is dependent on Adprt1a or Adprt2. Accumulation of Myc-APL in chromatin following exposure of *adprt1a*⁻ cells to cisplatin remains largely intact relative to *apl*⁻ cells (Fig. 5A and S3). Despite basal levels of APL in chromatin being less in *adprt2*⁻ and *adprt1a*⁻*adprt2*⁻ cells in the absence of cisplatin (Fig. 5A), these strains display a significant reduction in cisplatin-induced enrichment of APL in chromatin (Fig. 5A and S3), indicating Adprt2 is required to enrich and/or retain APL at DNA lesions induced by cisplatin.

Next we assessed whether the requirement for Adprt2 to assemble APL in chromatin following exposure to cisplatin is reflected in the ability of these cells to induce nuclear ADP-ribosylation following DNA damage. Compared to parental Ax2 cells, a slight but not significant decrease in ADP-ribosylation is apparent in *adprt1a*⁻ following exposure of cells to cisplatin. Surprisingly, despite a reduction in the ability of macrodomain-dependent

accumulation of APL in chromatin following exposure of *adprt2*⁻ cells to cisplatin (Figs 3B, 5A), robust nuclear ADP-ribosylation is apparent in these cells (Fig. 5B). However, this is dramatically reduced in the *adprt1a*⁻*adprt2*⁻ strain, indicating that whilst Adprt2 is required to signal cisplatin-induced DNA damage and promote assembly of APL in chromatin, in the absence of this ART Adprt1a signals this variety of DNA damage. Further evidence for this redundancy is provided by analysing the tolerance of *adprt1a*⁻, *adprt2*⁻, and *adprt1a*⁻*adprt2*⁻ strains to cisplatin treatment. Consistent with a lack of requirement for Adprt1a in producing ADP-ribosylation foci in response to cisplatin, *adprt1a*⁻ cells are no more sensitive to this genotoxin than parental Ax2 cells. However, the *adprt2*⁻ strain is sensitive to cisplatin to a similar degree to cells disrupted in *dclre1*, the *Dictyostelium* orthologue of SNM1A, a gene required for tolerance to ICLs in a variety of organisms (Dronkert et al., 2000; Henriques and Moustacchi, 1980; Wang et al., 2011). Interestingly, disruption of *adprt1a* in combination with *adprt2* further sensitises cells to cisplatin relative to the *adprt2*⁻ strain. Assessed collectively, these data suggest that at least two redundant, ART-dependent pathways operate in *Dictyostelium* in response to cisplatin: one mediated by Adprt2 and involving APL, and a secondary pathway dependent on Adprt1a.

Our previous work indicates that loss of Adprt2 results in increased DNA DSBs following exposure of cells to DNA alkylating agents and that this is subsequently signalled by Adprt1a to promote NHEJ and cell survival in response to these genotoxins (Couto et al., 2013). Given the redundancy between Adprt1a and Adprt2 in signalling cisplatin-induced DNA damage, we considered whether similar mechanisms are being employed in response to this variety of DNA damage. To test this hypothesis, we assessed the survival of NHEJ-deficient *dnapkcs*⁻ cells, *adprt2*⁻ cells and *adprt2*⁻*dnapkcs*⁻ cells to cisplatin treatment. Consistent with previous data, *adprt2*⁻ cells are sensitive to cisplatin treatment. Strikingly, whilst disruption of the *dnapkcs* gene alone has minimal impact on the sensitivity of Ax2 cells to cisplatin, the *adprt2*⁻*dnapkcs*⁻ strain is significantly more sensitive to cisplatin than *adprt2*⁻ cells (Fig. 5D). Taken together, these data reveal a role for NHEJ in the tolerance of cisplatin-induced DNA damage in the absence of Adprt2.

DISCUSSION

Our previous work identified that the ARTs Adprt2 and Adprt1b are required for tolerance of *Dictyostelium* cells to DNA SSBs, whilst Adprt1a is required to promote repair of DSBs by NHEJ (Couto et al., 2011). Adprt1a-mediated repair of DSBs is regulated, in part, through a PBZ domain in *Dictyostelium* Ku70 that is required to enrich the protein at sites of DNA damage. This domain is unusually prevalent in *Dictyostelium*, being apparent in a greater number of proteins implicated in the DDR than in humans, suggesting that ADP-ribose interaction domains may act as surrogate markers for novel DNA repair proteins (Ahel et al., 2008). Here we identify *Dictyostelium* proteins that contain the ADP-ribose binding macrodomain and characterise APL as a protein enriched in chromatin in response to the cisplatin in a manner that this is dependent on its macrodomain and the ART Adprt2.

The macrodomain of APL has undergone a circular permutation. This mutation is apparent in all dictyostelids in which the genomes have been sequenced. This rearrangement is not unique to *Dictyostelium*, with a similar permuted macrodomain being present in *Arabidopsis thaliana* and *Oryza sativa*. Structural analysis of this novel macrodomain indicates it has retained the core features of this domain family, including the $\alpha/\beta/\alpha$ sandwich fold consisting of a 6-stranded β -sheet flanked by α -helices (Rack et al., 2016). Moreover, several key amino acids within the ADP-ribose binding pocket that coordinate ADP-ribose binding are conserved in this domain. Most notably they retain an amino acid (D175/E439) at an equivalent position to D723 of human ALC1 (Ahel et al., 2009; Gottschalk et al., 2009) and D20 of *Archaeoglobus fulgidus* AF1521 (Karras et al., 2005) that is critical for ADP-ribose binding. Additionally, F113 that forms a binding pocket for the distal ribose unit is absolutely conserved and the two substrate binding loops (Loops 1 and 2) that flank the pyrophosphate of the ADP-ribose are also apparent (Ahel et al., 2009; Chen et al., 2011; Gottschalk et al., 2009; Karras et al., 2005). Consistent with the permuted macrodomain of *Dictyostelium* APL being able to interact with ADP-ribose, we observe that this domain is able to bind ADP-ribose polymers *in vitro* (Fig. 2D,E). Overall, these data indicate that whilst the macrodomain has undergone a circular permutation, it has retained its tertiary structure and its ability to interact with ADP-ribose.

APL contains several domains that suggest it plays a role in DNA repair. In addition to the macrodomain, it also contains a central PBZ domain. This motif is present in three human proteins, all of which are implicated in DNA repair (Ahel et al., 2008). Additionally, whilst the PBZ domain is more prevalent in *Dictyostelium*, all the proteins that contain this domain are implicated either in DNA repair directly (e.g. Ku70 and Ung), or the wider DDR (e.g. Rad17,

Chk2 and CHFR). Additionally, APL also contains an FHA domain at its N-terminus homologous to the FHA domain in other organisms that interact with the DNA repair proteins XRCC1 and XRCC4 (Ali et al., 2009; Bekker-Jensen et al., 2007; Iles et al., 2007; Loizou et al., 2004; Luo et al., 2004). These observations led us to speculate that APL may function in DNA repair. Consistent with this hypothesis, we observe that APL is enriched in chromatin following exposure of cells to cisplatin, an agent that induces DNA ICLs (Fig. 3A). Cisplatin is also able to induce DNA intra-strand crosslinks, primarily between neighbouring guanines, raising the possibility is that APL is detecting this variety of DNA damage, as opposed to ICLs (Eastman, 1983; Fichtinger-Schepman et al., 1985). Importantly, however, we do not observe enrichment of APL in chromatin following exposure of cells to agents that induce base damage repaired by BER (MMS), or bulky DNA adducts that are repaired by NER (4-NQO; Fig. 3A). Therefore, we believe that APL is responding to DNA ICLs, as opposed to other varieties of DNA damage induced by cisplatin.

Sequence analysis reveals no obvious motifs in APL that might perform a catalytic role in the processing or repair of DNA damage. Whilst a proportion of macrodomains are known to remove ADP-ribose moieties from proteins, as opposed to binding ADP-ribosylation (Barkauskaite et al., 2015; Jankevicius et al., 2013; Rosenthal et al., 2013; Sharifi et al., 2013; Slade et al., 2011), we have been unable to detect any such activity in APL (data not shown). Taken together, these data suggest a more structural role for APL in sensing signals induced by DNA ICLs, rather than direct modulation of DNA lesions. In this regard, the overall domain architecture of APL is similar to APLF, a vertebrate protein implicated promoting DNA strand break repair by facilitating accumulation of repair proteins at damage sites (Bekker-Jensen et al., 2007; Iles et al., 2007; Kanno et al., 2007; Rulten et al., 2008; Rulten et al., 2011). Whilst both proteins contain an N-terminal FHA domain and central PBZ domain, the C-terminal PBZ domain of APLF has been substituted for a macrodomain in APL. Macrodomains have been proposed to bind terminal ADP-ribose moieties within PAR chains (Karras et al., 2005), whilst PBZ domains bind the ADP-ribose-ADP-ribose junction and adenine rings internal to ADP-ribose polymers (Eustermann et al., 2010; Li et al., 2010; Oberoi et al., 2010). It is interesting to speculate, therefore, that the macrodomain and PBZ domain of APL might act in tandem to bind internally to the PAR chain and the terminal ADP-ribose unit respectively to facilitate high affinity binding to ADP-ribose polymers.

The occurrence of APL-like macrodomains in very distant organisms, such as *Dictyostelium* species and plants, suggests a general utility of this module to support DNA repair signalling. Of note, the APL macrodomain in plants is fused to two other DNA repair domains, aprataxin and polynucleotide kinase (Rack et al., 2016), strongly implying that APL supports DNA

repair in plants as well. Furthermore, as in vertebrate aprataxin, PNK as well as APLF are FHA domain-containing proteins that interact with DNA repair ligase complexes. Given the APLF domain structure is not preserved in plants and Dictyostelids (Mehrotra et al., 2011), it is tempting to speculate that APL may be supporting the PAR-binding function instead of APLF in these organisms.

Our data indicate a hitherto unrecognised role for ADP-ribosylation in the cellular response to cisplatin, an agent that induces DNA ICLs. This is based on our observations that a) robust nuclear ADP-ribosylation is observed in response to the ICL-inducing agent cisplatin, b) enrichment of APL in chromatin in response to cisplatin is dependent on its macrodomain and the ART Adprt2, and c) the *adprt2*⁻ strain is sensitive to cisplatin. Our data in *Dictyostelium* (Couto et al., 2013; Couto et al., 2011; Pears et al., 2012), in addition to those of others in vertebrates (Gibson and Kraus, 2012), implicate ARTs in repair of SSBs and DSBs. Therefore, it is possible that ARTs are detecting these or similar DNA architectures following processing of cisplatin-induced DNA damage, rather than the ICL directly. However, whilst Adprt2 is required for tolerance to DNA SSBs, the enrichment of APL in chromatin, an event that is dependent on Adprt2, does not occur in response to canonical base damage induced by MMS or 4-NQO. Similarly, no gross enrichment of APL is observed in chromatin following DNA DSBs and the Adprt2 strain is not sensitive to agents that induce this variety of DNA damage (Couto et al., 2013). Therefore, we believe Adprt2-mediated ADP-ribosylation induced by cisplatin is not induced by these DNA damage types directly, or if so, it is in the context of these DNA structures being produced as a consequence of DNA ICL processing.

Resolution of ICLs is facilitated by combining a number of repair pathways. In prokaryotes and lower eukaryotes such as budding yeast, repair is initiated by the nucleotide excision repair (NER) apparatus that incises adjacent to the ICL to ‘unhook’ the lesion. The Pso2 nuclease digests past the unhooked ICL, producing a gapped intermediate that is filled-in by translesion synthesis (TLS) using low fidelity DNA polymerases. The remaining crosslinked strand is removed by HR or a second round of NER (Dronkert and Kanaar, 2001; Lehoczky et al., 2007; Sengerova et al., 2011). Although a similar pathway has been proposed in mammalian cells (Ben-Yehoyada et al., 2009; Muniandy et al., 2009; Smeaton et al., 2008), the principal mechanism for ICL repair occurs during S-phase and is coordinated by the Fanconi Anaemia (FA) pathway (Kottemann and Smogorzewska, 2013). ICLs result in stalling of replication forks that are detected by the FA core complex. The FANCL component of this complex ubiquitylates FANCD2/FANCI, which serves as a platform to coordinate a number of downstream factors. These include the nuclease FAN1, and SLX4

that acts as a scaffold for other nucleases including XPF, Mus81 and SLX1. Following incision either side of the ICL on one DNA strand, in addition to potential processing by Pso2/SNM1A, TLS bypasses the lesion. If replication forks have converged on the ICL, this process results in a DSB that is repaired by HR. In the absence of replication fork convergence, the remaining ICL is either removed by NER, or TLS results in a one-sided DSB that is resolved by HR (Sengerova et al., 2011).

Dictyostelium shares the core components of all pathways implicated in repair of ICLs, including the FA pathway (dictybase.org) (Hsu et al., 2011; Lee et al., 1998; Lee et al., 1997; McVey, 2010; Yu et al., 1998; Zhang et al., 2009). It is possible that Adprt2 could be acting at any stage of these pathways. For example, it could directly detect DNA ICLs, either during S-phase, or another stage of the cell cycle. Alternatively, as alluded to above, it could signal other DNA architectures resulting from processing of ICLs, most notably gapped single-stranded DNA intermediates and/or DNA DSBs. In this regard, Adprt2 functions analogous to vertebrate PARP1, being required for tolerance to DNA SSBs, but playing a minor role in promoting NHEJ (Couto et al., 2011). Given PARP1 has also been implicated in promoting the re-start of damaged/stalled replication forks (Bryant et al., 2009; Sugimura et al., 2008; Yang et al., 2004), it is interesting to speculate that Adprt2 and ADP-ribosylation may be acting in a similar pathway, although in the context of repairing damaged replication forks that encounter DNA ICLs. It should be noted however, that during vegetative cell growth *Dictyostelium* cells have no discernible G1, with approximately 10% of cells undergoing DNA replication, and the majority being in G2 phase of the cell cycle (Couto et al., 2013; Muramoto and Chubb, 2008; Weijer et al., 1984). Given up to 80% of cells display ADP-ribosylation foci following cisplatin treatment (Fig. 4B), this might indicate an S-phase independent role for Adprt2-mediated ADP-ribosylation in DNA ICL repair. In this regard, *Dictyostelium* FA mutants display only mild sensitivity to ICLs, whilst an *xpf* strain is extremely sensitive to this variety of DNA damage (Zhang et al., 2009). Furthermore, ADP-ribosylation has previously been implicated in resolution of UV-induced DNA damage by NER, a pathway that acts independently of S-phase (Fischer et al., 2014; Pines et al., 2012; Robu et al., 2013). It will therefore be interesting to more formally assess whether Adprt2 functions in conjunction with the FA pathway during DNA replication, or might be involved in an excision repair pathway at other stages of the cell cycle.

Although *adprt2*⁻ cells display sensitivity to cisplatin, robust nuclear ADP-ribosylation is evident in these cells that is dependent on Adprt1a. Taken together, these data indicate that whilst Adprt2 is required for tolerance to cisplatin, in its absence Adprt1a can signal DNA damage to maintain cell viability in the face of DNA damage. Redundancy exists between

ARTs in signalling DNA damage. For example, PARP1 and PARP2 both respond to DNA base damage and redundancy between these ARTs has been implied by the embryonic lethality of *parp1^{-/-}parp2^{-/-}* mice (Menissier de Murcia et al., 2003). Moreover, PARP1 and PARP3, the functional orthologues of *Dictyostelium* Adprt2 and Adprt1a respectively, act synergistically in response to IR in mouse and human cells (Boehler et al., 2011). Our observations of redundancy between Adprt2 and Adprt1a in signalling cisplatin-induced DNA damage is reminiscent of the situation in signalling DNA base damage in *Dictyostelium*. In the absence of Adprt2, SSBs are converted to DSBs that are subsequently signalled by Adprt1a to promote NHEJ (Couto et al., 2013). Consistent with a similar scenario occurring in response to cisplatin, we observe that disruption of NHEJ in combination with Adprt2 also further sensitises cells to cisplatin, indicating that NHEJ is a functional pathway in ICL repair in *Dictyostelium* providing tolerance of these lesions in the absence of Adprt2. Whilst a defective FA pathway can channel repair through NHEJ the impact on cell viability is variable depending on the organism studied, or the NHEJ components disrupted. For example, disruption of the NHEJ pathway in *C. elegans* and humans suppresses the sensitivity of FA mutants to ICLs (Adamo et al., 2010). A similar reversal of ICL sensitivity is also observed in FA-defective chicken DT40 cells when disrupting *Ku70*, although this is not the case when disrupting other NHEJ factors such as DNA-PKcs or Ligase IV (Pace et al., 2010). In contrast, experiments using mouse embryonic fibroblasts indicate that disruption of *fancd2* and *ku80* or *53bp1* in combination increases genome instability and sensitivity to ICLs (Bunting et al., 2012; Houghtaling et al., 2005). Our data indicating that disruption of Adprt2 and NHEJ in combination further sensitises cells to cisplatin suggests that similar to the studies in mice, in the absence of effective ICL repair NHEJ performs a beneficial role in allowing cells to tolerate agents such as cisplatin. One potential explanation for these data is the cell cycle distribution of vegetative *Dictyostelium* cells. For example, NHEJ is generally toxic during S-phase, whilst it is effectively utilised in G2 (Beucher et al., 2009; Rothkamm et al., 2003). Given the majority of *Dictyostelium* cells are in G2 during vegetative cell growth, it is conceivable that loss of effective ICL repair and subsequent engagement of NHEJ is beneficial in this stage of the cell cycle.

In summary, our search for novel macrodomain containing proteins identified APL as a factor that is able to interact with ADP-ribose polymers *in vitro*. The presence of FHA and macrodomains in this protein implicate it in the cellular response to DNA damage and consistent with this hypothesis, we observe that APL is enriched in chromatin specifically in response to an agent that induces DNA ICLs. The dependence of this event on the macrodomain of APL implicates ADP-ribosylation in this response, and consistent with this hypothesis we find that the ART Adprt2 is required to ADP-ribosylate proteins in response to

cisplatin exposure. Furthermore, in the absence of Adprt2, we uncover a role for NHEJ in allowing cells to tolerate cisplatin. Taken together, these data illustrate redundancy between ARTs that signal alternate varieties of DNA damage to maintain cell viability in the face of genotoxic stress.

MATERIALS AND METHODS

Homology searching and multiple sequence alignments

In silico searches were performed within dictyBase (www.dictybase.org) and the non-redundant UniRef50 database (Basu et al., 2015; Wu et al., 2006). Proteins containing known macrodomains were identified in the Pfam and SUPERFAMILY protein databases (Finn et al., 2016; Wilson et al., 2009). Initial local homology searches were formed using BLAST (Altschul et al., 1997). Profile hidden Markov models (profile-HMMs) were generated using HMMer2 and HMMer3, which were also used for profile-sequence homology searches, which were iterated up to 40 times (Eddy, 1996; Finn et al., 2011). HHpred was employed for profile-profile homology searches (Soding et al., 2005). Secondary structure predictions were performed with PsiPred (Jones, 1999).

Protein amino acid sequences were obtained from UniProt or dictyBase (Basu et al., 2015; Wu et al., 2006). Alignments of protein sequences were performed using MUSCLE or T-Coffee, and visualised in Belvu (Edgar, 2004; Notredame et al., 2000; Sonnhammer and Hollich, 2005). DNA sequences were aligned using the MultAlin interface (Corpet, 1988).

Protein expression and purification

GST-tagged proteins were generated by amplifying the following regions of the *apl* gene from cDNA and ligation into pGEX-4T-1 (GE Healthcare): GST-APL (nucleotides 1-1689), GST-FHA (nucleotides 1-336), GST-PBZ (nucleotides 504-591), GST-MACRO (nucleotides 1026-1689). GST-tagged proteins were expressed and purified according to the manufacturer's instructions. Selenomethionine-substituted *D. discoideum* macrodomain protein was produced with SelenoMet Medium Base and Nutrient Mix (Molecular Dimensions) as per manufacturer's instructions and purified as above.

Crystallisation, data collection and processing

Crystallization trials were performed with proteins at 25 mg/ml in buffer containing 150 mM NaCl, 1 mM DTT and 25 mM Tris-HCl (pH 7.5), at 20°C with commercial screens using the sitting-drop vapour-diffusion method. Crystallization drops were set up with the aid of a Mosquito Crystal robot (TTP Labtech) using 200 nl of protein solution plus 200 nl of reservoir solution in MRC two-well crystallization microplates (Swissci) equilibrated against 75 µl of

reservoir solution. Co-crystallisation trials were set up by adding 2 mM ADPr to the protein for at least 1 hour prior to setting up crystallisation drops. Crystals of the macrodomain proteins grew in 0.2 M Lithium sulphate, 0.1 M phosphate/citrate and 20% (w/v) PEG1000 (*Dictyostelium*), and in 0.1 M SPG buffer pH 4 (succinic acid, sodium phosphate monobasic monohydrate and glycine) and 25% (w/v) PEG 1500 (*O. sativa*). Crystals were cryoprotected by transfer into reservoir solution before being vitrified by submersion in liquid nitrogen. X-ray data were collected at beamlines I04 of the Diamond Light Source (Rutherford Appleton Laboratory, Harwell, UK) and data collection statistics are shown in Table 1. X-ray data were processed using Xia2 (Winter et al., 2013). *Dictyostelium* macrodomain X-ray data was phased with AUTOSOL (Terwilliger et al., 2009). PHASER (Storoni et al., 2004) was used to solve the *O. sativa* macrodomain data by molecular replacement with the *Dictyostelium* macrodomain structure. Model building for all structures was carried out with COOT (Emsley and Cowtan, 2004) and real space refinement with REFMAC5 (Murshudov et al., 1997), coupled with automatically generated local non-crystallographic symmetry restraints. Structural figures were prepared using PyMOL (Molecular Graphics System, Version 1.3 Schrödinger, LLC).

PAR-binding assays

GST-tagged proteins were serially diluted and increasing concentrations between 0.625 pmol to 2.5 pmol of proteins were either slot-blotted or dot-blotted onto a nitrocellulose. The membrane was blocked with 5% milk in TBS-T, before incubation with PAR polymers (Trevigen). The membrane is then washed with TBS-T, followed by 4 washes with TBS-T with 1 M NaCl, and a further wash with TBS-T. Detection was performed by Western blotting with Anti-PAR (Trevigen) and Anti-GST (Sigma-Aldrich) antibodies.

Cell culture and strain generation

Dictyostelium cells were grown according to standard procedures, either axenically or on SM agar plates in association with *Klebsiella aerogenes*. Generation of the *adprt1a*⁻, *adprt2*⁻, *adprt1a*⁻/*adprt2*⁻, *dnapkcs*⁻, *dnapkcs*⁻/*adprt2*⁻ and *dclre1*⁻ cells has been previously described (Couto et al., 2013; Couto et al., 2011; Hudson et al., 2005). To generate an *apl*⁻ strain, DNA fragments upstream (nucleotides -1,031 to -3) and downstream (nucleotides +1916 to +2,849) of the *apl* gene were amplified by PCR and ligated into the pLPBLP vector (dictyBase) to flank a blasticidin resistance cassette (Faix et al., 2004). The disruption construct was excised from the pLPBLP vector by restriction digestion with HpaI/NotI, and was transfected into Ax2 cells using standard procedures. Blasticidin was added the following day at a concentration of 10 µg/ml to provide selection. Blasticidin-resistant clones were isolated and screened for *apl* disruption by PCR and Southern blotting (Fig. S2).

To express Myc-APL in *Dictyostelium* strains, the cDNA sequence of full length APL or Myc-APL-Δ342-563 was amplified by PCR, utilising primers to introduce an in-frame N-terminal Myc-tag, and ligated into pDXA-3C (dictyBase). Plasmids were electroporated into *Dictyostelium* cells alongside the pREP helper plasmid (dictyBase) according to standard procedures. Cells expressing Myc-APL were selected for by addition of 10 µg/ml G418 (Sigma-Aldrich) after 24 hours.

Subcellular fractionation

Exponentially growing *Dictyostelium* cells were resuspended to a density of 5×10^6 cells/ml in HL5 and incubated with genotoxic agents (Sigma-Aldrich). For MMS, phleomycin and 4-NQO, incubation was for 1 hour (4-NQO-treated cells were incubated in the dark). For cisplatin, cells were resuspended to 5×10^6 cells/ml in Pt buffer (1 mM NaPO₄, 3 mM NaCl, pH 6.5) and incubated in the dark for 5 hours. Following incubation, the cells were washed with KK2 and resuspended in nuclear lysis buffer (50 mM HEPES, pH 7.5, 150 mM NaCl, 1 mM EDTA, phosphatase inhibitor cocktail 2 & 3 [Sigma-Aldrich], proteasome inhibitor cocktail [Roche], 10 mM benzamide [Sigma-Aldrich], 200 µM DEA [Trevigen]) with 0.1% Triton X-100 to a density of 5×10^6 cells/ml. Cells were incubated on ice for 15 minutes, before centrifugation at 14,000 ×g for 3 minutes at 4°C. The pellet was resuspended in the same volume of nuclear lysis buffer with 0.1% Triton X-100, and incubated on ice for 15 minutes, before centrifugation at 14,000 ×g for 3 minutes at 4°C. The pellet was resuspended in nuclear lysis buffer with 200 µg/ml RNase A (Sigma-Aldrich), and incubated for 30 minutes at room temperature with rotation, before centrifugation as above. The final pellet is resuspended in 2× SDS loading buffer containing 100 µM DTT prior to boiling for 5 minutes. Whole-cell extracts were prepared by washing cells in KK2, and resuspending in 2× SDS loading buffer containing 100 µM DTT, prior to boiling for 5 minutes.

Analysis of extracts was performed by SDS-PAGE and Western blotting with the following primary antibodies: Anti-Myc (Santa Cruz), Anti-H3 (Abcam), Anti-γH2AX, Anti-Actin (Santa Cruz) Anti-pan-ADP-ribose binding reagent (MABE1016, Millipore).

Immunofluorescence

Exponentially growing *Dictyostelium* cells were resuspended to a density of 1×10^6 cells/ml in HL5 and allowed to adhere to glass coverslips for 30 minutes. The HL5 was then removed and the coverslips washed with Pt buffer. Cells were then exposed to 300 µM cisplatin for the indicated times, in the dark. Coverslips were incubated for 5 minutes in ice-cold nuclear extraction buffer (10 mM PIPES, pH 6.8, 300 mM sucrose, 3 mM MgCl₂, 20 mM NaCl, 0.5%

Triton X-100) and washed twice with TBS. Cells were fixed with ice cold 70% ethanol for 5 minutes, followed by the addition and immediate removal of ice-cold 100% methanol, prior to washing thrice with TBS.

Coverslips were blocked with 3% BSA in TBS for 1 hour, prior to a 2 hour incubation with an Anti-pan-ADP-ribose binding reagent (MABE1016; Millipore) in 3% BSA. Coverslips were washed three times in TBS, then incubated in the dark for 1 hour with a TRIT-C-conjugated anti-rabbit secondary antibody (R0156; Dako), followed by three further TBS washes. Coverslips were mounted onto glass slides using VECTASHIELD mounting media containing DAPI (Vector Laboratories) and visualized with a microscope (1X71; Olympus). 250 nuclei were analysed per condition. Images were acquired on a camera using HCImage Acquisition (Hamamatsu Photonics) image software and processed in Photoshop (Adobe).

DNA damage survival assays

Exponentially growing *Dictyostelium* cells were resuspended to 1×10^6 cells/ml in Pt buffer, and exposed to the indicated concentrations of cisplatin (Sigma-Aldrich). Cells were incubated in shaking suspension at 100 rpm for 5 hours in the dark. 1×10^4 cells were diluted 1:100 in KK2 and 250 cells mixed with 350 μ l *K. aerogenes* and transferred to 140 mm SM agar plates in duplicate. The plates were incubated in the dark and survival assessed by observing plaque formation after 3, 4, 5 and 6 days.

ACKNOWLEDGEMENTS

We thank Catherine Pears and members of the Lakin and Pears laboratories for constructive comments during the course of this work and preparation of the manuscript.

COMPETING INTERESTS

No competing interests declared.

AUTHOR CONTRIBUTIONS

A.R.G. and L.S.P. performed the bioinformatics analysis and homology modelling in the laboratory of C. P. B.B.P. purified and crystallised proteins for the structural studies. The structures were solved by A.A. and D.L. ADP-ribose binding experiments were performed by P.P., M.E. and B.B.P. Experiments assessing the role of ARTs in cisplatin induced ADP-ribosylation were performed by A.R.G. and J.D. The manuscript was written by N.D.L, A.R.G. and I.A.

FUNDING

Work in N.D.L.'s laboratory is supported by Cancer Research UK (www.cancerresearch.org.uk; grant C1521/A12353), Medical Research Council (www.mrc.ac.uk; MR/L000164/1) and NC3Rs (www.nc3rs.org.uk; NC/K00137X/1). A.R.G. was supported by the EPSRC Systems Biology Doctoral Training Centre, University of Oxford and the EPAbraham Cephalosporin Trust Fund. Work in the I.A. laboratory is supported by Wellcome Trust (www.wellcome.ac.uk; grant number 101794) and European Research Council (www.erc.europa.eu; grant number 281739).

REFERENCES

- Adamo, A., Collis, S. J., Adelman, C. A., Silva, N., Horejsi, Z., Ward, J. D., Martinez-Perez, E., Boulton, S. J. and La Volpe, A. (2010). Preventing nonhomologous end joining suppresses DNA repair defects of Fanconi anemia. *Mol Cell* **39**, 25-35.
- Ahel, D., Horejsi, Z., Wiechens, N., Polo, S. E., Garcia-Wilson, E., Ahel, I., Flynn, H., Skehel, M., West, S. C., Jackson, S. P. et al. (2009). Poly(ADP-ribose)-dependent regulation of DNA repair by the chromatin remodeling enzyme ALC1. *Science* **325**, 1240-3.
- Ahel, I., Ahel, D., Matsusaka, T., Clark, A. J., Pines, J., Boulton, S. J. and West, S. C. (2008). Poly(ADP-ribose)-binding zinc finger motifs in DNA repair/checkpoint proteins. *Nature* **451**, 81-5.
- Ali, A. A., Jukes, R. M., Pearl, L. H. and Oliver, A. W. (2009). Specific recognition of a multiply phosphorylated motif in the DNA repair scaffold XRCC1 by the FHA domain of human PNK. *Nucleic Acids Res* **37**, 1701-12.
- Altschul, S. F., Madden, T. L., Schaffer, A. A., Zhang, J., Zhang, Z., Miller, W. and Lipman, D. J. (1997). Gapped BLAST and PSI-BLAST: a new generation of protein database search programs. *Nucleic Acids Res* **25**, 3389-402.
- Ame, J. C., Rolli, V., Schreiber, V., Niedergang, C., Apiou, F., Decker, P., Muller, S., Hoger, T., Murcia, J. M. D. and de Murcia, G. (1999). PARP-2, a novel mammalian DNA damage-dependent poly(ADP-ribose) polymerase. *Journal of Biological Chemistry* **274**, 17860-17868.
- Audebert, M., Salles, B. and Calsou, P. (2004). Involvement of poly(ADP-ribose) polymerase-1 and XRCC1/DNA ligase III in an alternative route for DNA double-strand breaks rejoining. *J Biol Chem* **279**, 55117-26.
- Barkauskaite, E., Jankevicius, G. and Ahel, I. (2015). Structures and Mechanisms of Enzymes Employed in the Synthesis and Degradation of PARP-Dependent Protein ADP-Ribosylation. *Mol Cell* **58**, 935-46.
- Basu, S., Fey, P., Jimenez-Morales, D., Dodson, R. J. and Chisholm, R. L. (2015). dictyBase 2015: Expanding data and annotations in a new software environment. *Genesis* **53**, 523-34.
- Bekker-Jensen, S., Fugger, K., Danielsen, J. R., Gromova, I., Sehested, M., Celis, J., Bartek, J., Lukas, J. and Mailand, N. (2007). Human Xip1 (C2orf13) is a novel regulator of cellular responses to DNA strand breaks. *J Biol Chem* **282**, 19638-43.
- Ben-Yehoyada, M., Wang, L. C., Kozekov, I. D., Rizzo, C. J., Gottesman, M. E. and Gautier, J. (2009). Checkpoint signaling from a single DNA interstrand crosslink. *Mol Cell* **35**, 704-15.
- Beucher, A., Birraux, J., Tchouandong, L., Barton, O., Shibata, A., Conrad, S., Goodarzi, A. A., Krempler, A., Jeggo, P. A. and Lobrich, M. (2009). ATM and Artemis promote homologous recombination of radiation-induced DNA double-strand breaks in G2. *Embo J* **28**, 3413-27.
- Block, W. D. and Lees-Miller, S. P. (2005). Putative homologues of the DNA-dependent protein kinase catalytic subunit (DNA-PKcs) and other components of the non-homologous end joining machinery in Dictyostelium discoideum. *DNA Repair (Amst)* **4**, 1061-5.
- Boehler, C., Gauthier, L. R., Mortusewicz, O., Biard, D. S., Saliou, J. M., Bresson, A., Sanglier-Cianferani, S., Smith, S., Schreiber, V., Boussin, F. et al. (2011). Poly(ADP-ribose) polymerase 3 (PARP3), a newcomer in cellular response to DNA damage and mitotic progression. *Proc Natl Acad Sci U S A* **108**, 2783-8.
- Brown, M. L., Franco, D., Burkle, A. and Chang, Y. (2002). Role of poly(ADP-ribosylation) in DNA-PKcs- independent V(D)J recombination. *Proc Natl Acad Sci U S A* **99**, 4532-7.
- Bryant, H. E., Petermann, E., Schultz, N., Jemth, A. S., Loseva, O., Issaeva, N., Johansson, F., Fernandez, S., McGlynn, P. and Helleday, T. (2009). PARP is activated at stalled forks to mediate Mre11-dependent replication restart and recombination. *Embo J* **28**, 2601-15.

Bunting, S. F., Callen, E., Kozak, M. L., Kim, J. M., Wong, N., Lopez-Contreras, A. J., Ludwig, T., Baer, R., Faryabi, R. B., Malhowski, A. et al. (2012). BRCA1 functions independently of homologous recombination in DNA interstrand crosslink repair. *Mol Cell* **46**, 125-35.

Caldecott, K. W. (2008). Single-strand break repair and genetic disease. *Nat Rev Genet* **9**, 619-31.

Chappell, C., Hanakahi, L. A., Karimi-Busheri, F., Weinfeld, M. and West, S. C. (2002). Involvement of human polynucleotide kinase in double-strand break repair by non-homologous end joining. *Embo J* **21**, 2827-32.

Chen, D., Vollmar, M., Rossi, M. N., Phillips, C., Kraehenbuehl, R., Slade, D., Mehrotra, P. V., von Delft, F., Crosthwaite, S. K., Gileadi, O. et al. (2011). Identification of macrodomain proteins as novel O-acetyl-ADP-ribose deacetylases. *J Biol Chem* **286**, 13261-71.

Clements, P. M., Breslin, C., Deeks, E. D., Byrd, P. J., Ju, L., Bieganowski, P., Brenner, C., Moreira, M. C., Taylor, A. M. and Caldecott, K. W. (2004). The ataxia-oculomotor apraxia 1 gene product has a role distinct from ATM and interacts with the DNA strand break repair proteins XRCC1 and XRCC4. *DNA Repair (Amst)* **3**, 1493-502.

Corpet, F. (1988). Multiple sequence alignment with hierarchical clustering. *Nucleic Acids Res* **16**, 10881-90.

Couto, C. A., Hsu, D. W., Teo, R., Rakhimova, A., Lempidaki, S., Pears, C. J. and Lakin, N. D. (2013). Nonhomologous end-joining promotes resistance to DNA damage in the absence of an ADP-ribosyltransferase that signals DNA single strand breaks. *J Cell Sci* **126**, 3452-61.

Couto, C. A., Wang, H. Y., Green, J. C., Kiely, R., Siddaway, R., Borer, C., Pears, C. J. and Lakin, N. D. (2011). PARP regulates nonhomologous end joining through retention of Ku at double-strand breaks. *J Cell Biol* **194**, 367-75.

de Murcia, J. M., Niedergang, C., Trucco, C., Ricoul, M., Dutrillaux, B., Mark, M., Oliver, F. J., Masson, M., Dierich, A., LeMeur, M. et al. (1997). Requirement of poly(ADP-ribose) polymerase in recovery from DNA damage in mice and in cells. *Proceedings of the National Academy of Sciences of the United States of America* **94**, 7303-7307.

Ding, R., Pommier, Y., Kang, V. H. and Smulson, M. (1992). Depletion of poly(ADP-ribose) polymerase by antisense RNA expression results in a delay in DNA strand break rejoining. *J Biol Chem* **267**, 12804-12.

Dronkert, M. L. G. and Kanaar, R. (2001). Repair of DNA interstrand cross-links. *Mutation Research-DNA Repair* **486**, 217-247.

Eastman, A. (1983). Characterization of the adducts produced in DNA by cis-diamminedichloroplatinum(II) and cis-dichloro(ethylenediamine)platinum(II). *Biochemistry* **22**, 3927-33.

Eddy, S. R. (1996). Hidden Markov models. *Curr Opin Struct Biol* **6**, 361-5.

Eddy, S. R. (1998). Profile hidden Markov models. *Bioinformatics* **14**, 755-63.

Edgar, R. C. (2004). MUSCLE: multiple sequence alignment with high accuracy and high throughput. *Nucleic Acids Res* **32**, 1792-7.

Emsley, P. and Cowtan, K. (2004). Coot: model-building tools for molecular graphics. *Acta Crystallogr D Biol Crystallogr* **60**, 2126-32.

Eustermann, S., Brockmann, C., Mehrotra, P. V., Yang, J. C., Loakes, D., West, S. C., Ahel, I. and Neuhaus, D. (2010). Solution structures of the two PBZ domains from human APLF and their interaction with poly(ADP-ribose). *Nat Struct Mol Biol* **17**, 241-3.

Faix, J., Kreppel, L., Shaulsky, G., Schleicher, M. and Kimmel, A. R. (2004). A rapid and efficient method to generate multiple gene disruptions in *Dictyostelium discoideum* using a single selectable marker and the Cre-loxP system. *Nucleic Acids Res* **32**, e143.

Fichtinger-Schepman, A. M., van der Veer, J. L., den Hartog, J. H., Lohman, P. H. and Reedijk, J. (1985). Adducts of the antitumor drug cis-diamminedichloroplatinum(II) with DNA: formation, identification, and quantitation. *Biochemistry* **24**, 707-13.

Finn, R. D., Clements, J. and Eddy, S. R. (2011). HMMER web server: interactive sequence similarity searching. *Nucleic Acids Res* **39**, W29-37.

Finn, R. D., Coggill, P., Eberhardt, R. Y., Eddy, S. R., Mistry, J., Mitchell, A. L., Potter, S. C., Punta, M., Qureshi, M., Sangrador-Vegas, A. et al. (2016). The Pfam protein families database: towards a more sustainable future. *Nucleic Acids Res* **44**, D279-85.

Fischer, J. M., Popp, O., Gebhard, D., Veith, S., Fischbach, A., Beneke, S., Leitenstorfer, A., Bergemann, J., Scheffner, M., Ferrando-May, E. et al. (2014). Poly(ADP-ribose)-mediated interplay of XPA and PARP1 leads to reciprocal regulation of protein function. *Febs J* **281**, 3625-41.

Fisher, A. E., Hochegger, H., Takeda, S. and Caldecott, K. W. (2007). Poly(ADP-ribose) polymerase 1 accelerates single-strand break repair in concert with poly(ADP-ribose) glycohydrolase. *Mol Cell Biol* **27**, 5597-605.

Gagne, J. P., Isabelle, M., Lo, K. S., Bourassa, S., Hendzel, M. J., Dawson, V. L., Dawson, T. M. and Poirier, G. G. (2008). Proteome-wide identification of poly(ADP-ribose) binding proteins and poly(ADP-ribose)-associated protein complexes. *Nucleic Acids Res* **36**, 6959-76.

Gibson, B. A. and Kraus, W. L. (2012). New insights into the molecular and cellular functions of poly(ADP-ribose) and PARPs. *Nat Rev Mol Cell Biol* **13**, 411-24.

Gottschalk, A. J., Timinszky, G., Kong, S. E., Jin, J., Cai, Y., Swanson, S. K., Washburn, M. P., Florens, L., Ladurner, A. G., Conaway, J. W. et al. (2009). Poly(ADP-ribosyl)ation directs recruitment and activation of an ATP-dependent chromatin remodeler. *Proc Natl Acad Sci U S A* **106**, 13770-4.

Hottiger, M. O., Hassa, P. O., Luscher, B., Schuler, H. and Koch-Nolte, F. (2010). Toward a unified nomenclature for mammalian ADP-ribosyltransferases. *Trends Biochem Sci* **35**, 208-19.

Houghtaling, S., Newell, A., Akkari, Y., Taniguchi, T., Olson, S. and Grompe, M. (2005). Fancd2 functions in a double strand break repair pathway that is distinct from non-homologous end joining. *Hum Mol Genet* **14**, 3027-33.

Hsu, D. W., Gaudet, P., Hudson, J. J., Pears, C. J. and Lakin, N. D. (2006). DNA damage signaling and repair in Dictyostelium discoideum. *Cell Cycle* **5**, 702-8.

Hsu, D. W., Kiely, R., Couto, C. A., Wang, H. Y., Hudson, J. J., Borer, C., Pears, C. J. and Lakin, N. D. (2011). DNA double-strand break repair pathway choice in Dictyostelium. *J Cell Sci* **124**, 1655-63.

Hudson, J. J., Hsu, D. W., Guo, K., Zhukovskaya, N., Liu, P. H., Williams, J. G., Pears, C. J. and Lakin, N. D. (2005). DNA-PKcs-dependent signaling of DNA damage in Dictyostelium discoideum. *Curr Biol* **15**, 1880-5.

Iles, N., Rulten, S., El-Khamisy, S. F. and Caldecott, K. W. (2007). APLF (C2orf13) is a novel human protein involved in the cellular response to chromosomal DNA strand breaks. *Mol Cell Biol* **27**, 3793-803.

Jankevicius, G., Hassler, M., Golia, B., Rybin, V., Zacharias, M., Timinszky, G. and Ladurner, A. G. (2013). A family of macrodomain proteins reverses cellular mono-ADP-ribosylation. *Nat Struct Mol Biol* **20**, 508-14.

Jones, D. T. (1999). Protein secondary structure prediction based on position-specific scoring matrices. *J Mol Biol* **292**, 195-202.

Kanno, S., Kuzuoka, H., Sasao, S., Hong, Z., Lan, L., Nakajima, S. and Yasui, A. (2007). A novel human AP endonuclease with conserved zinc-finger-like motifs involved in DNA strand break responses. *Embo J* **26**, 2094-103.

Karras, G. I., Kustatscher, G., Buhecha, H. R., Allen, M. D., Pugieux, C., Sait, F., Bycroft, M. and Ladurner, A. G. (2005). The macro domain is an ADP-ribose binding module. *Embo J* **24**, 1911-20.

Kottemann, M. C. and Smogorzewska, A. (2013). Fanconi anaemia and the repair of Watson and Crick DNA crosslinks. *Nature* **493**, 356-63.

Krishnakumar, R. and Kraus, W. L. (2010). The PARP side of the nucleus: molecular actions, physiological outcomes, and clinical targets. *Mol Cell* **39**, 8-24.

Le Page, F., Schreiber, V., Dherin, C., De Murcia, G. and Boiteux, S. (2003). Poly(ADP-ribose) polymerase-1 (PARP-1) is required in murine cell lines for base excision repair of oxidative DNA damage in the absence of DNA polymerase beta. *J Biol Chem* **278**, 18471-7.

Lee, S. K., Yu, S. L., Alexander, H. and Alexander, S. (1998). A mutation in repB, the dictyostelium homolog of the human xeroderma pigmentosum B gene, has increased sensitivity to UV-light but normal morphogenesis. *Biochim Biophys Acta* **1399**, 161-72.

Lee, S. K., Yu, S. L., Garcia, M. X., Alexander, H. and Alexander, S. (1997). Differential developmental expression of the rep B and rep D xeroderma pigmentosum related DNA helicase genes from Dictyostelium discoideum. *Nucleic Acids Res* **25**, 2365-74.

Lehoczky, P., McHugh, P. J. and Chovanec, M. (2007). DNA interstrand cross-link repair in *Saccharomyces cerevisiae*. *FEMS Microbiol Rev* **31**, 109-33.

Li, G. Y., McCulloch, R. D., Fenton, A. L., Cheung, M., Meng, L., Ikura, M. and Koch, C. A. (2010). Structure and identification of ADP-ribose recognition motifs of APLF and role in the DNA damage response. *Proc Natl Acad Sci U S A* **107**, 9129-34.

Loizou, J. I., El-Khamisy, S. F., Zlatanou, A., Moore, D. J., Chan, D. W., Qin, J., Sarno, S., Meggio, F., Pinna, L. A. and Caldecott, K. W. (2004). The protein kinase CK2 facilitates repair of chromosomal DNA single-strand breaks. *Cell* **117**, 17-28.

Loseva, O., Jemth, A. S., Bryant, H. E., Schuler, H., Lehtio, L., Karlberg, T. and Helleday, T. (2010). PARP-3 is a mono-ADP-ribosylase that activates PARP-1 in the absence of DNA. *J Biol Chem* **285**, 8054-60.

Luijsterburg, M. S., de Krijger, I., Wiegant, W. W., Shah, R. G., Smeenk, G., de Groot, A. J., Pines, A., Vertegaal, A. C., Jacobs, J. J., Shah, G. M. et al. (2016). PARP1 Links CHD2-Mediated Chromatin Expansion and H3.3 Deposition to DNA Repair by Non-homologous End-Joining. *Mol Cell* **61**, 547-62.

Luo, H., Chan, D. W., Yang, T., Rodriguez, M., Chen, B. P., Leng, M., Mu, J. J., Chen, D., Songyang, Z., Wang, Y. et al. (2004). A new XRCC1-containing complex and its role in cellular survival of methyl methanesulfonate treatment. *Mol Cell Biol* **24**, 8356-65.

Masutani, M., Nozaki, T., Nishiyama, E., Shimokawa, T., Tachi, Y., Suzuki, H., Nakagama, H., Wakabayashi, K. and Sugimura, T. (1999). Function of poly(ADP-ribose)polymerase in response to DNA damage: Gene-disruption study in mice. *Molecular and Cellular Biochemistry* **193**, 149-152.

McVey, M. (2010). Strategies for DNA interstrand crosslink repair: insights from worms, flies, frogs, and slime molds. *Environ Mol Mutagen* **51**, 646-58.

Mehrotra, P. V., Ahel, D., Ryan, D. P., Weston, R., Wiechens, N., Kraehenbuehl, R., Owen-Hughes, T. and Ahel, I. (2011). DNA repair factor APLF is a histone chaperone. *Mol Cell* **41**, 46-55.

Menissier de Murcia, J., Ricoul, M., Tartier, L., Niedergang, C., Huber, A., Dantzer, F., Schreiber, V., Ame, J. C., Dierich, A., LeMeur, M. et al. (2003). Functional interaction between PARP-1 and PARP-2 in chromosome stability and embryonic development in mouse. *Embo J* **22**, 2255-63.

Messner, S. and Hottiger, M. O. (2011). Histone ADP-ribosylation in DNA repair, replication and transcription. *Trends Cell Biol* **21**, 534-42.

Muniandy, P. A., Thapa, D., Thazhathveetil, A. K., Liu, S. T. and Seidman, M. M. (2009). Repair of laser-localized DNA interstrand cross-links in G1 phase mammalian cells. *J Biol Chem* **284**, 27908-17.

Muramoto, T. and Chubb, J. R. (2008). Live imaging of the Dictyostelium cell cycle reveals widespread S phase during development, a G2 bias in spore differentiation and a premitotic checkpoint. *Development* **135**, 1647-57.

Murshudov, G. N., Vagin, A. A. and Dodson, E. J. (1997). Refinement of macromolecular structures by the maximum-likelihood method. *Acta Crystallogr D Biol Crystallogr* **53**, 240-55.

Nicolae, C. M., Aho, E. R., Choe, K. N., Constantin, D., Hu, H. J., Lee, D., Myung, K. and Moldovan, G. L. (2015). A novel role for the mono-ADP-ribosyltransferase PARP14/ARTD8 in promoting homologous recombination and protecting against replication stress. *Nucleic Acids Res* **43**, 3143-53.

Notredame, C., Higgins, D. G. and Heringa, J. (2000). T-Coffee: A novel method for fast and accurate multiple sequence alignment. *J Mol Biol* **302**, 205-17.

Oberoi, J., Richards, M. W., Crumpler, S., Brown, N., Blagg, J. and Bayliss, R. (2010). Structural basis of poly(ADP-ribose) recognition by the multizinc binding domain of checkpoint with forkhead-associated and RING Domains (CHFR). *J Biol Chem* **285**, 39348-58.

Pace, P., Mosedale, G., Hodkinson, M. R., Rosado, I. V., Sivasubramaniam, M. and Patel, K. J. (2010). Ku70 corrupts DNA repair in the absence of the Fanconi anemia pathway. *Science* **329**, 219-23.

Pears, C. J., Couto, C. A., Wang, H. Y., Borer, C., Kiely, R. and Lakin, N. D. (2012). The role of ADP-ribosylation in regulating DNA double-strand break repair. *Cell Cycle* **11**, 48-56.

Pines, A., Vrouwe, M. G., Marteijn, J. A., Typas, D., Luijsterburg, M. S., Cansoy, M., Hensbergen, P., Deelder, A., de Groot, A., Matsumoto, S. et al. (2012). PARP1 promotes nucleotide excision repair through DDB2 stabilization and recruitment of ALC1. *J Cell Biol* **199**, 235-49.

Ponting, C. P. and Russell, R. B. (1995). Swaposins: circular permutations within genes encoding saposin homologues. *Trends Biochem Sci* **20**, 179-80.

Quenet, D., El Ramy, R., Schreiber, V. and Dantzer, F. (2009). The role of poly(ADP-ribosylation) in epigenetic events. *Int J Biochem Cell Biol* **41**, 60-5.

Rack, J. G., Perina, D. and Ahel, I. (2016). Macrodomains: Structure, Function, Evolution, and Catalytic Activities. *Annu Rev Biochem*.

Robert, I., Dantzer, F. and Reina-San-Martin, B. (2009). Parp1 facilitates alternative NHEJ, whereas Parp2 suppresses IgH/c-myc translocations during immunoglobulin class switch recombination. *J Exp Med* **206**, 1047-56.

Robu, M., Shah, R. G., Petitclerc, N., Brind'Amour, J., Kandan-Kulangara, F. and Shah, G. M. (2013). Role of poly(ADP-ribose) polymerase-1 in the removal of UV-induced DNA lesions by nucleotide excision repair. *Proc Natl Acad Sci U S A* **110**, 1658-63.

Rosenthal, F., Feijs, K. L., Frugier, E., Bonalli, M., Forst, A. H., Imhof, R., Winkler, H. C., Fischer, D., Caflisch, A., Hassa, P. O. et al. (2013). Macrodomain-containing proteins are new mono-ADP-ribosylhydrolases. *Nat Struct Mol Biol* **20**, 502-7.

Rothkamm, K., Kruger, I., Thompson, L. H. and Lobrich, M. (2003). Pathways of DNA double-strand break repair during the mammalian cell cycle. *Mol Cell Biol* **23**, 5706-15.

Rulten, S. L., Cortes-Ledesma, F., Guo, L., Iles, N. J. and Caldecott, K. W. (2008). APLF (C2orf13) is a novel component of poly(ADP-ribose) signaling in mammalian cells. *Mol Cell Biol* **28**, 4620-8.

Rulten, S. L., Fisher, A. E., Robert, I., Zuma, M. C., Rouleau, M., Ju, L., Poirier, G., Reina-San-Martin, B. and Caldecott, K. W. (2011). PARP-3 and APLF function together to accelerate nonhomologous end-joining. *Mol Cell* **41**, 33-45.

Schreiber, V., Ame, J. C., Dolle, P., Schultz, I., Rinaldi, B., Fraulob, V., Menissier-de Murcia, J. and de Murcia, G. (2002). Poly(ADP-ribose) polymerase-2 (PARP-2) is required for efficient base excision DNA repair in association with PARP-1 and XRCC1. *J Biol Chem* **277**, 23028-36.

Sengerova, B., Wang, A. T. and McHugh, P. J. (2011). Orchestrating the nucleases involved in DNA interstrand cross-link (ICL) repair. *Cell Cycle* **10**, 3999-4008.

Sharifi, R., Morra, R., Denise Appel, C., Tallis, M., Chioza, B., Jankevicius, G., Simpson, M. A., Matic, I., Ozkan, E., Golia, B. et al. (2013). Deficiency of terminal ADP-ribose protein glycohydrolase TARG1/C6orf130 in neurodegenerative disease. *Embo J*.

Slade, D., Dunstan, M. S., Barkauskaite, E., Weston, R., Lafite, P., Dixon, N., Ahel, M., Leys, D. and Ahel, I. (2011). The structure and catalytic mechanism of a poly(ADP-ribose) glycohydrolase. *Nature* **477**, 616-20.

Smeaton, M. B., Hlavin, E. M., McGregor Mason, T., Noronha, A. M., Wilds, C. J. and Miller, P. S. (2008). Distortion-dependent unhooking of interstrand cross-links in mammalian cell extracts. *Biochemistry* **47**, 9920-30.

Soding, J., Biegert, A. and Lupas, A. N. (2005). The HHpred interactive server for protein homology detection and structure prediction. *Nucleic Acids Res* **33**, W244-8.

Sonnhammer, E. L. and Hollich, V. (2005). Scoredist: a simple and robust protein sequence distance estimator. *BMC Bioinformatics* **6**, 108.

Storoni, L. C., McCoy, A. J. and Read, R. J. (2004). Likelihood-enhanced fast rotation functions. *Acta Crystallogr D Biol Crystallogr* **60**, 432-8.

Sugimura, K., Takebayashi, S., Taguchi, H., Takeda, S. and Okumura, K. (2008). PARP-1 ensures regulation of replication fork progression by homologous recombination on damaged DNA. *J Cell Biol* **183**, 1203-12.

Terwilliger, T. C., Adams, P. D., Read, R. J., McCoy, A. J., Moriarty, N. W., Grosse-Kunstleve, R. W., Afonine, P. V., Zwart, P. H. and Hung, L. W. (2009). Decision-making in structure solution using Bayesian estimates of map quality: the PHENIX AutoSol wizard. *Acta Crystallogr D Biol Crystallogr* **65**, 582-601.

Timinszky, G., Till, S., Hassa, P. O., Hothorn, M., Kustatscher, G., Nijmeijer, B., Colombelli, J., Altmeyer, M., Stelzer, E. H., Scheffzek, K. et al. (2009). A macrodomain-containing histone rearranges chromatin upon sensing PARP1 activation. *Nat Struct Mol Biol* **16**, 923-9.

Trucco, C., Oliver, F. J., de Murcia, G. and Menissier-de Murcia, J. (1998). DNA repair defect in poly(ADP-ribose) polymerase-deficient cell lines. *Nucleic Acids Research* **26**, 2644-2649.

Vyas, S., Matic, I., Uchima, L., Rood, J., Zaja, R., Hay, R. T., Ahel, I. and Chang, P. (2014). Family-wide analysis of poly(ADP-ribose) polymerase activity. *Nat Commun* **5**, 4426.

Wang, M., Wu, W., Rosidi, B., Zhang, L., Wang, H. and Iliakis, G. (2006). PARP-1 and Ku compete for repair of DNA double strand breaks by distinct NHEJ pathways. *Nucleic Acids Res* **34**, 6170-82.

Weijer, C. J., Duschl, G. and David, C. N. (1984). A revision of the Dictyostelium discoideum cell cycle. *J Cell Sci* **70**, 111-31.

Wilson, D., Pethica, R., Zhou, Y., Talbot, C., Vogel, C., Madera, M., Chothia, C. and Gough, J. (2009). SUPERFAMILY--sophisticated comparative genomics, data mining, visualization and phylogeny. *Nucleic Acids Res* **37**, D380-6.

Winter, G., Lobley, C. M. and Prince, S. M. (2013). Decision making in xia2. *Acta Crystallogr D Biol Crystallogr* **69**, 1260-73.

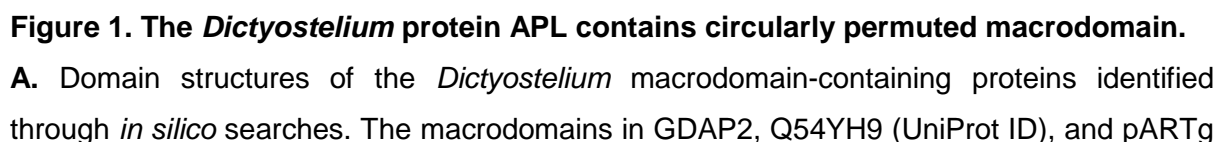
Wu, C. H., Apweiler, R., Bairoch, A., Natale, D. A., Barker, W. C., Boeckmann, B., Ferro, S., Gasteiger, E., Huang, H., Lopez, R. et al. (2006). The Universal Protein Resource (UniProt): an expanding universe of protein information. *Nucleic Acids Res* **34**, D187-91.

Yang, Y. G., Cortes, U., Patnaik, S., Jasin, M. and Wang, Z. Q. (2004). Ablation of PARP-1 does not interfere with the repair of DNA double-strand breaks, but compromises the reactivation of stalled replication forks. *Oncogene* **23**, 3872-82.

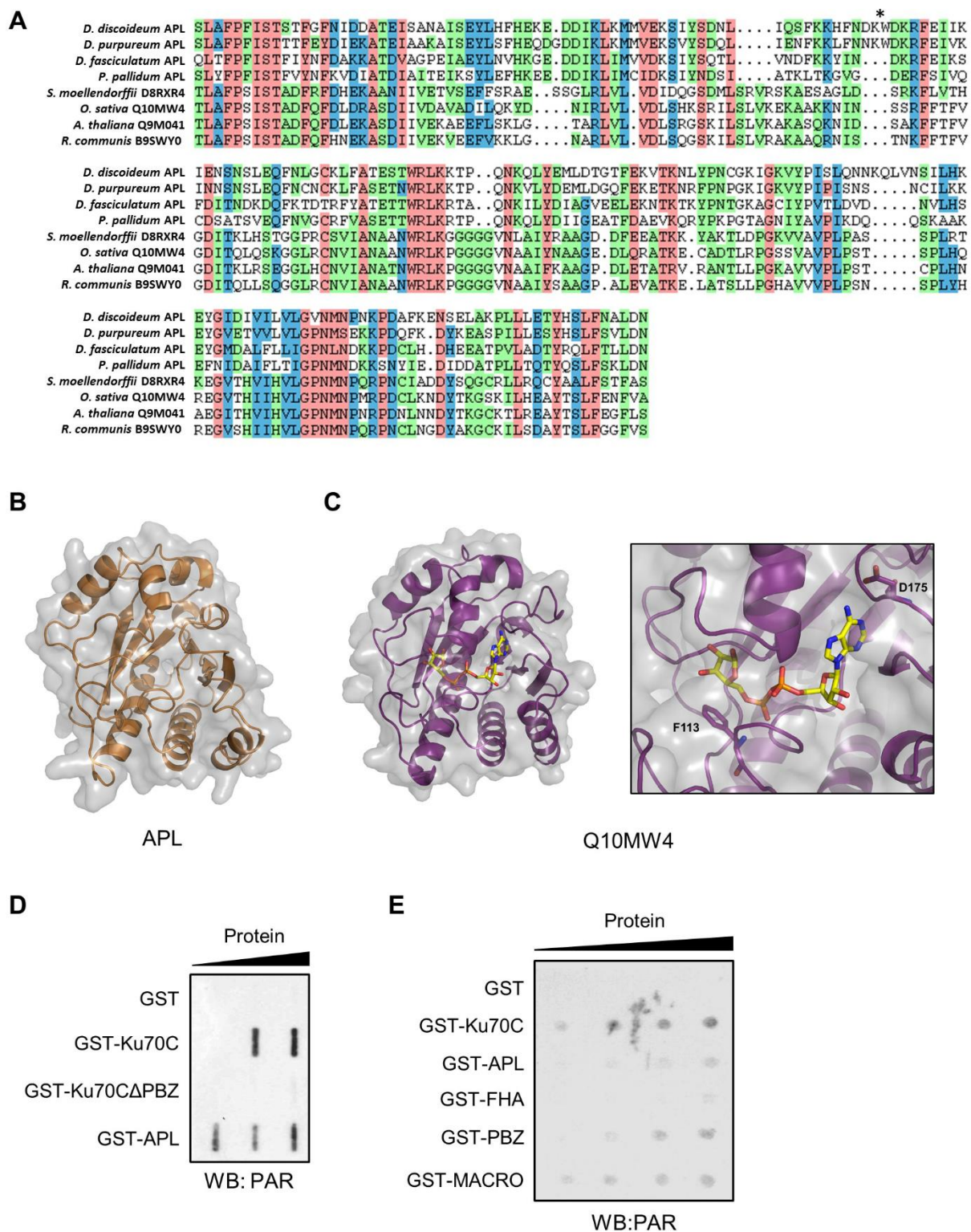
Yu, S. L., Lee, S. K., Alexander, H. and Alexander, S. (1998). Rapid changes of nucleotide excision repair gene expression following UV-irradiation and cisplatin treatment of Dictyostelium discoideum. *Nucleic Acids Res* **26**, 3397-403.

Zhang, X. Y., Langenick, J., Traynor, D., Babu, M. M., Kay, R. R. and Patel, K. J. (2009). Xpf and not the Fanconi anaemia proteins or Rev3 accounts for the extreme resistance to cisplatin in Dictyostelium discoideum. *PLoS Genet* **5**, e1000645.

Journal of Cell Science • Advance article



were previously annotated. Domain abbreviations: forkhead-associated (FHA), zinc finger CCHH-type (PBZ), BRCA1 C-terminus (BRCT), CRAL-TRIO lipid binding domain (CRAL-TRIO), U-box domain (U-BOX), PARP catalytic domain (PARP). **B.** Multiple sequence alignment of APL from different dictyostelids, highlighting the domain conservation between the proteins. This alignment shows the conservation of a circularly permuted macrodomain, which is illustrated relative to the standard macrodomain. Circular permutation is likely to have arisen from the duplication of the C- and N-terminal regions of successive macro domains. For this to occur macro domains would need to occur in tandem in the progenitor protein, as indeed they do in many extant macro domain-containing proteins. In the circularly permuted macrodomain, the N- and C- termini of the standard macrodomain lie in the middle of the domain sequence.



dictyostelid orthologs of APL, or by UniProt accession number. The permutation site is marked by an asterisk. **B.** Crystal structure of the permuted macrodomain from *Dictyostelium* APL. **C.** Crystal structure of the permuted macrodomain from *O. sativa* Q10MW4 in a complex with ADP-ribose. A focus on the binding pocket of the permuted macrodomain indicates amino acids predicted to facilitate ADP-ribose binding and specificity: Phe-113 and Asp-175. **D.** *In vitro* PAR-binding activity of APL. The indicated recombinant GST-tagged proteins were slot-blotted onto a nitrocellulose membrane in increasing concentrations, prior to incubation of the membrane with PAR polymers. Detection of bound PAR was performed by Western blotting an Anti-PAR antibody. **E.** *In vitro* PAR-binding activity of the isolated domains of *Dictyostelium* APL. The indicated GST-tagged proteins were dot-blotted onto a nitrocellulose membrane, prior to incubation with PAR polymers and detection by Western blotting as in (D).

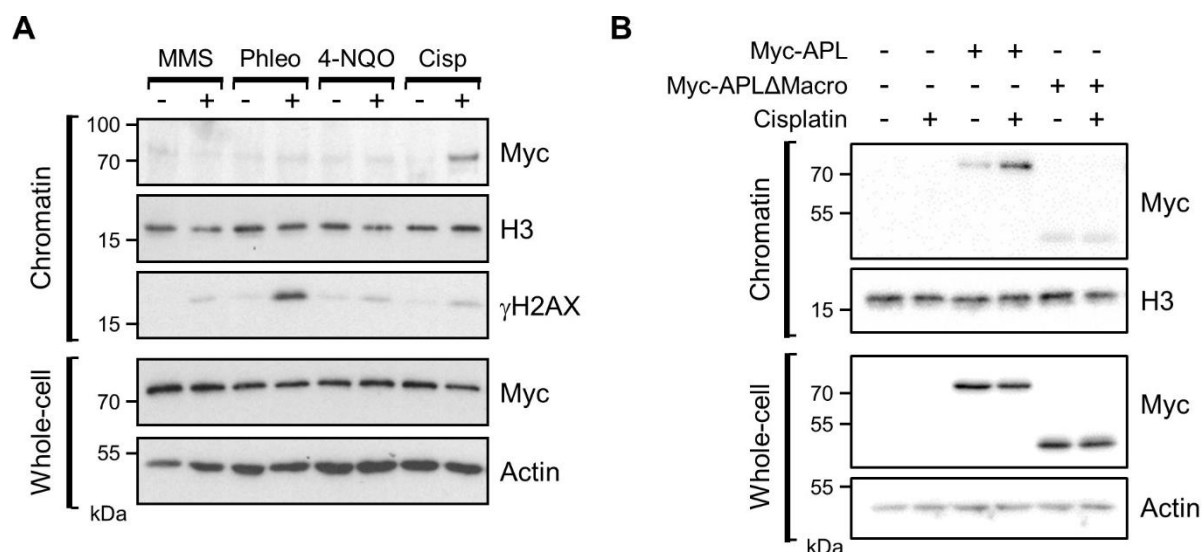


Figure 3. APL is enriched on chromatin following cellular exposure to cisplatin, in a manner dependent on its macrodomain.

A. *Dictyostelium apt* cells expressing Myc-APL were treated with the indicated DNA damaging agents and chromatin or whole-cell extracts prepared. Western blotting was performed with the indicated antibodies. **B.** *Dictyostelium apt* cells expressing full-length Myc-tagged APL (Myc-APL), or a form of APL with its macrodomain deleted (Myc-APL-ΔMacro), were exposed to cisplatin alongside cells transfected with an empty vector. Chromatin fractions and whole-cell extracts were prepared and Western blotting performed with the indicated antibodies. The image shown is representative of four independent experiments.

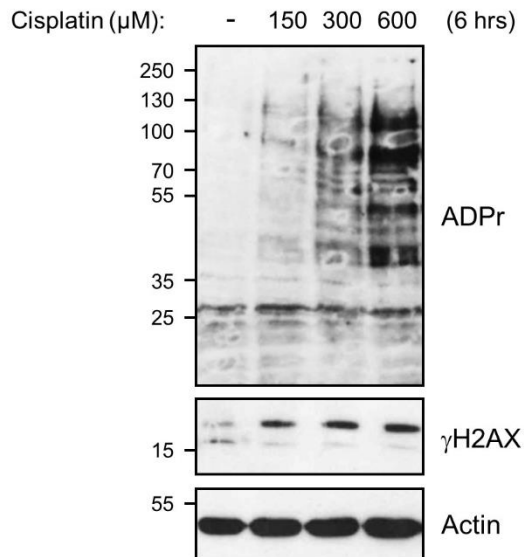
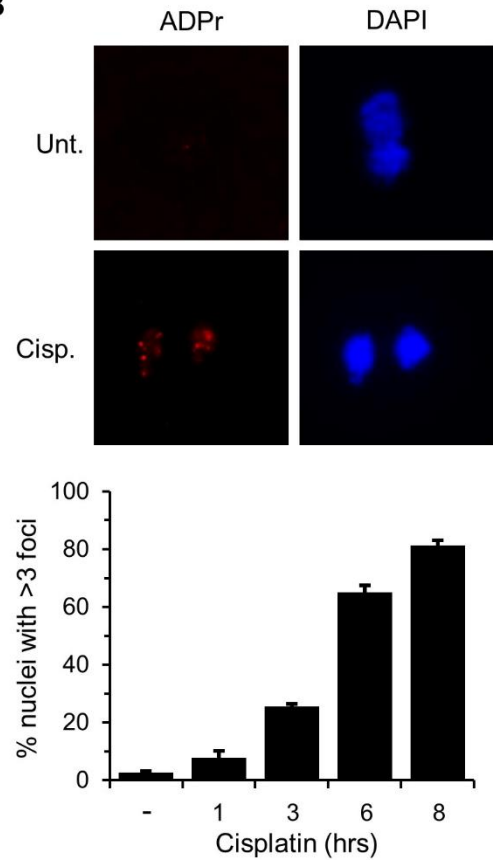
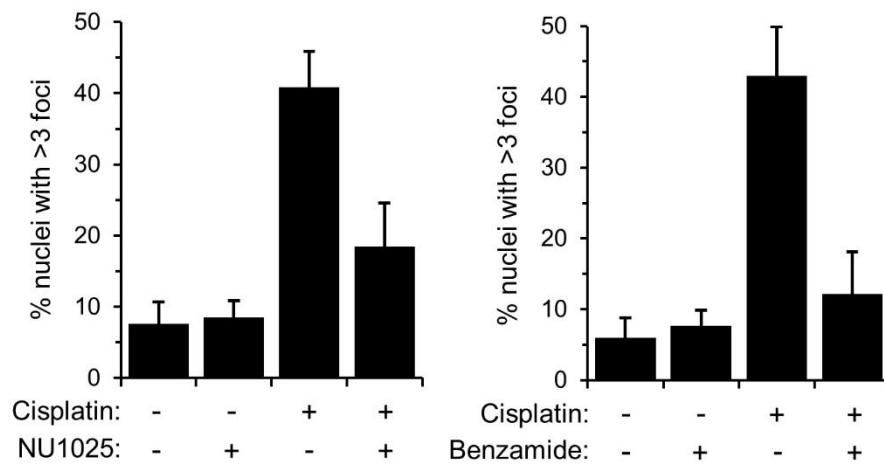
A**B****C**

Figure 4. Nuclear ADP-ribosylation is induced following cisplatin treatment.

A. *Dictyostelium* Ax2 cells were exposed to the indicated concentrations of cisplatin for 6 hours prior to preparation of whole-cell extracts. Western blotting was performed with the indicated antibodies. **B.** Ax2 cells were treated with 300 μM cisplatin for 6 hours, prior to nuclear extraction and staining with the indicated reagents for immunofluorescence. Images are representative of 250 nuclei. Error bars represent the s.e.m. from three independent

experiments. **C.** Quantification of the effect of treatment of PARP inhibitors, NU1025 and benzamide, on nuclear ADPr foci formation resulting from cisplatin exposure. Error bars represent the s.e.m. from four independent experiments.

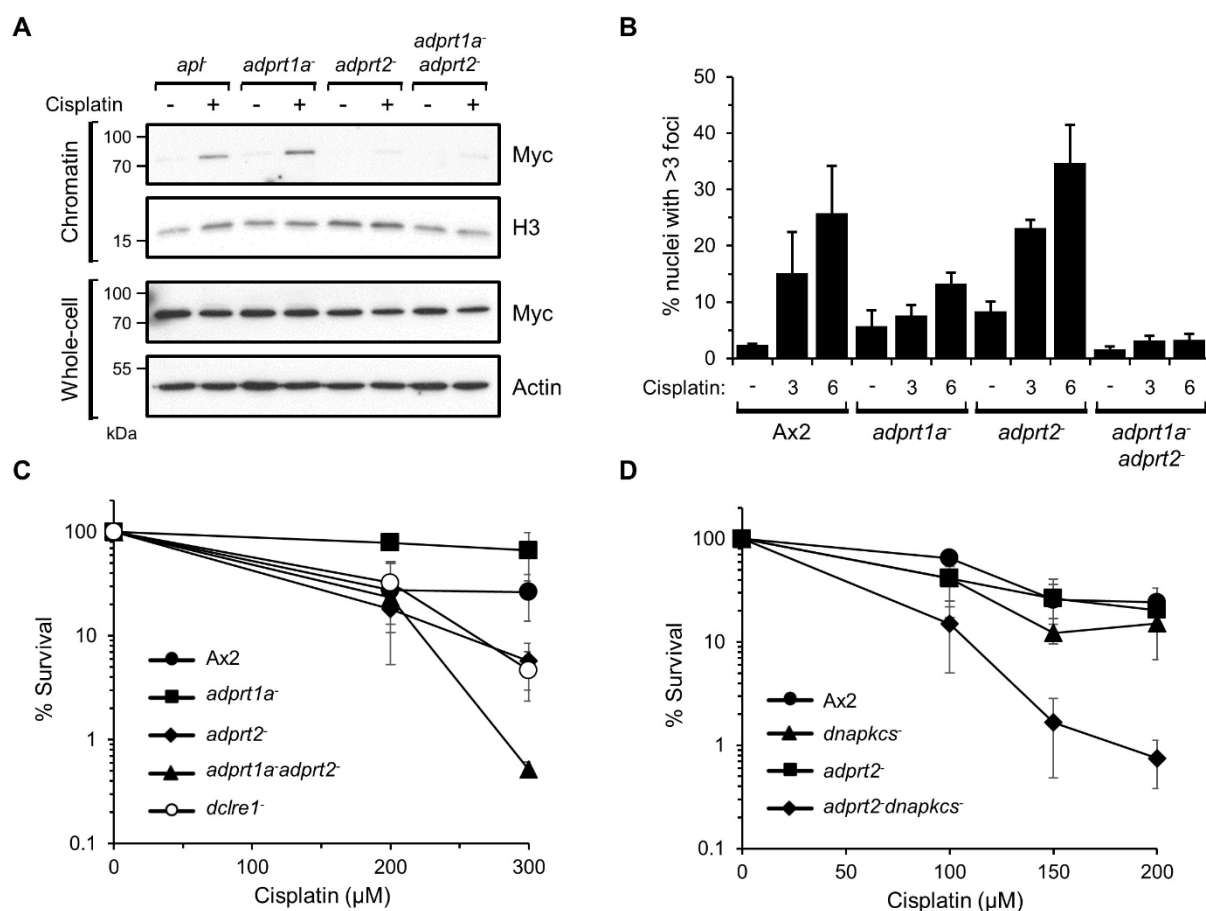


Figure 5. NHEJ provides resistance to interstrand crosslinks in the absence of Adprt2.

A. *Dictyostelium adprt1a*⁻, *adprt2*⁻ and *adprt1a adprt2*⁻ cells expressing Myc-APL were left untreated, or exposed to 300 μM cisplatin for 5 hours. Chromatin and whole-cell extracts were prepared and Western blotting performed with the indicated antibodies. The image shown is representative of three independent experiments. **B.** *Ax2*, *adprt1a*⁻, *adprt2*⁻, *adprt1a adprt2*⁻ cells were exposed to 300 μM cisplatin for 6 hours, prior to nuclear extraction and staining for immunofluorescence. Error bars represent the s.e.m. from three independent experiments. **C.** *Ax2*, *adprt1a*⁻, *adprt2*⁻, *adprt1a adprt2*⁻ cells were assessed for survival to the indicated concentrations of cisplatin. Error bars represent the s.e.m. from three independent experiments. **D.** *Ax2*, *dnapkcs*⁻, *adprt2*⁻ and *adprt2 dnapkcs*⁻ cells were assessed for survival to the indicated concentrations of cisplatin. Error bars represent the s.e.m. from four independent experiments.

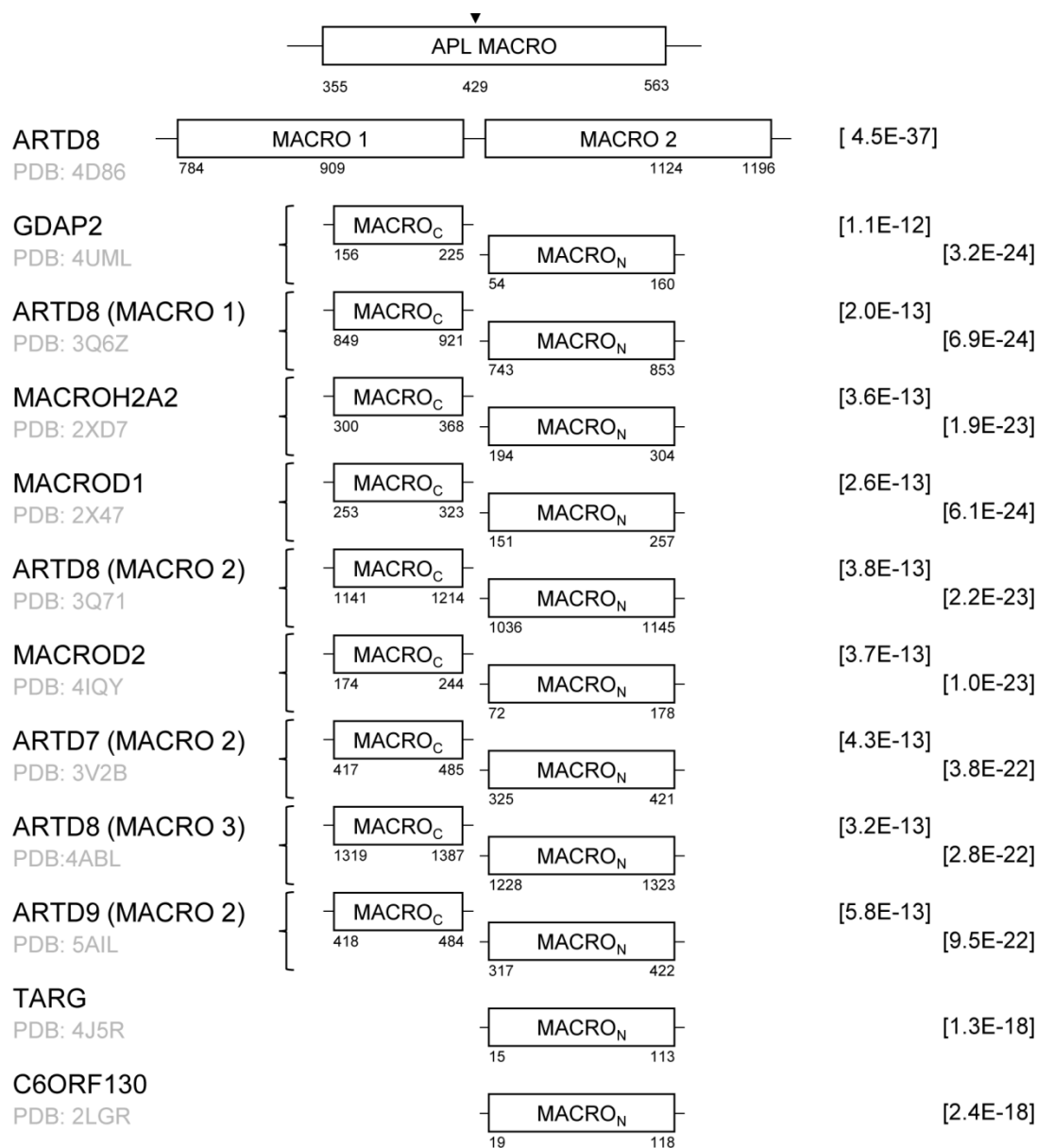


Figure S1. The macro domain of APL is circularly permuted. Graphical representation of the results from a HHPred search with the sequence of the macro domain of *Dictyostelium* APL as an input. The macro domain of APL is shown aligned to the solved structures of human macro domains. The circular permutation is indicated by the N (MACRO_N) and C (MACRO_C) terminal regions of the human macro domains aligning in a discontinuous manner. In the case of ARTD8, APL aligns at the centre of two adjacent macro domains. The values provided in square brackets are the E-values for each result.

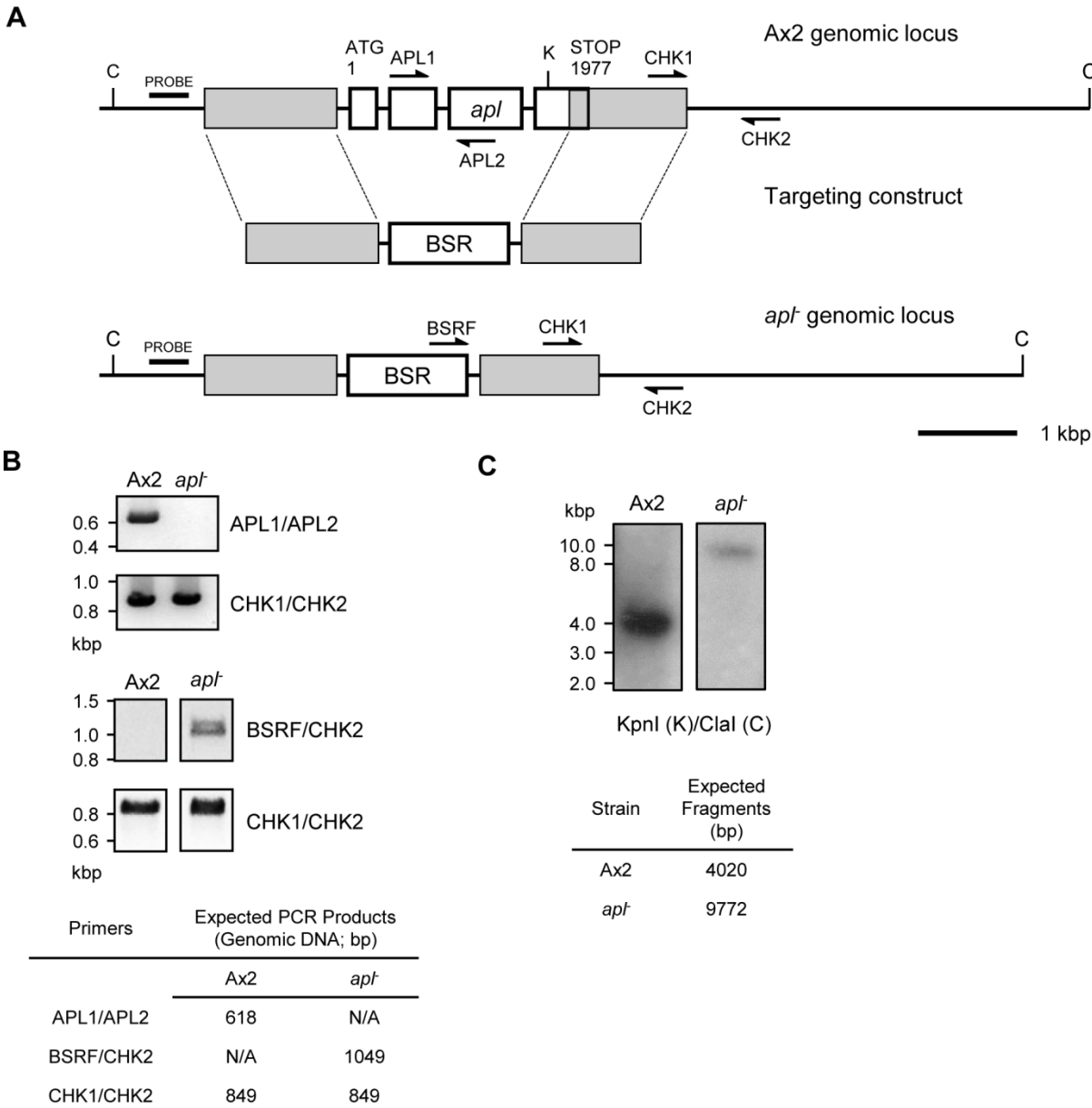


Figure S2. Generation and verification of an *apt* strain.

A. Strategy for the generation of an *apt* strain by targeted homologous recombination. The *apl* genomic locus is shown in parental Ax2 cells (top) and *apt* cells (bottom). Regions of homology in the targeting construct (middle) are depicted as grey boxes. This strategy results in disruption of the entire *apl* gene, with only the last 60 bases remaining of the final exon (white boxes). **B.** PCR verification of the *apt* strain using the primers at locations indicated in (A). The expected PCR product sizes for Ax2 and *apt* cells are given in the table. **C.** Southern blot verification of the *apt* strain. Digestion of Ax2 and *apt* genomic DNA with Clal (C) and KpnI (K) and using the probe indicated in (A) results in detection of the DNA fragments indicated in the table.

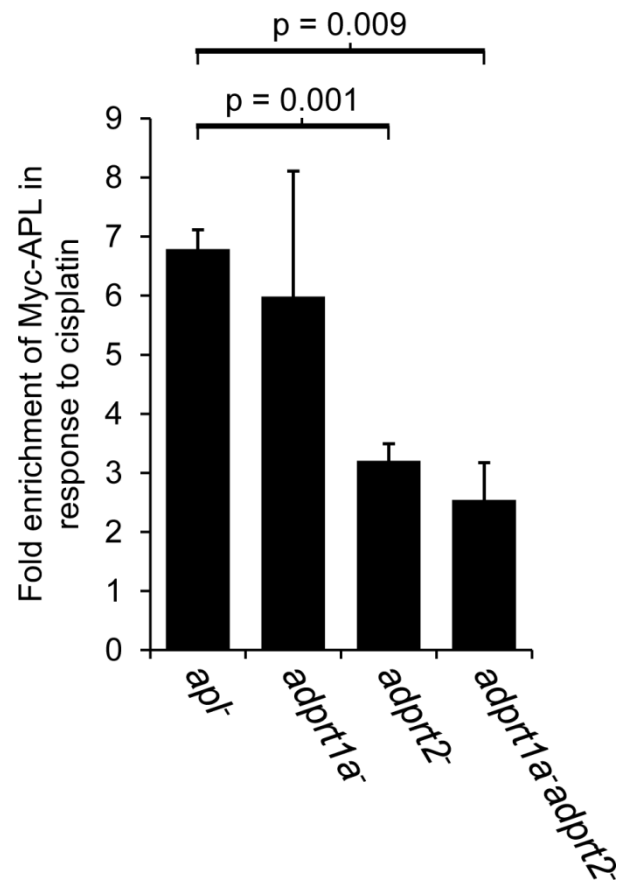


Figure S3. Quantification of APL enrichment in chromatin after administration of cisplatin to Ax2, *adprt1a*⁻, *adprt2*⁻ and *adprt1a adprt2*⁻ cells. *Dictyostelium apt*⁻, *adprt1a*⁻, *adprt2*⁻, and *adprt1a adprt2*⁻ cells were exposed to 300 μ M cisplatin for 5 hours, prior to chromatin extraction and analysis by Western blotting. Myc-APL levels detected in chromatin fractions were quantified using the Odyssey FC system (LI-COR). The Myc-APL signal was normalised to histone H3 levels. The data is presented as a fold enrichment of Myc-APL in cisplatin-treated cells compared to untreated cells. Error bars represent the s.e.m. from three independent experiments.

Table S1. Structural data, phasing and refinement statistics.

	Q10MW4 Macro	APL Macro
Data Collection		
Wavelength (Å)/beam line	0.9795/I04	0.9787/i24
Detector	Pilatus 6M-F	Pilatus 6M-F
Space group	C2	P2 ₁ 2 ₁ 2 ₁
a (Å)	73.50	39.59
b (Å)	91.32	71.22
c (Å)	62.88	81.89
α (°)	90.00	90.00
β (°)	103.32	90.00
γ (°)	90.00	90.00
Content of asymmetric unit	2	1
Resolution (Å)	56.31–1.66 (1.68–1.65)	25.19–1.80 (1.85–1.80)
R _{sym} (%) ^b	8.0 (40.6)	7.8 (94.3)
I/σ(I)	12.8 (3.2)	17.3 (5.3)
Completeness (%)	97.4 (77.7)	99.9 (100)
Redundancy	6.7 (5.2)	25.8 (25.4)
CC _{1/2} (%)	(87.5)	(98.2)
Number of unique reflections	47191 (1867)	22050 (1584)
Refinement		
R _{cryst} (%) ^c	15.5	17.0
R _{free} (%) ^d	18.7	21.4
Rmsd bond length (Å)	0.021	0.020
Rmsd bond angle (°)	1.56	1.90
Number of atoms		
Protein	3201	1798
Water	365	120
Phosphate ion	3	0
Glycine	2	0
ADP-ribose	2	0
Average B factor (Å²)		
Protein	23.8	19.5
Water	34.7	24.9
Chloride ion	47.2	N/A
Glycerol	54.7	N/A
ADP-ribose	26.6	N/A
Ramachandran plot		
Favoured	97.4	94.91
Allowed	2.6	3.70
Disallowed	0	1.39